

Electronic Supplementary Information (ESI†)

Phosphate based New Organic Polymer Networks for Efficient Dye Sorption and Catalyst Loading for Chemo-selective Reactivity

Shabari Dutta,^a Suman Kalyan Samanta*,^b and Santanu Bhattacharya*^{a,c}

^a School of Applied and Interdisciplinary Sciences, Indian Association for the Cultivation of Science, Kolkata 700032, India. E-mail: santanu.bhattacharya@iacs.res.in

^b Department of Chemistry, Indian Institute of Technology Kharagpur, Kharagpur 721302, India. E-mail: sksamanta@chem.iitkgp.ac.in

^c Department of Organic Chemistry, Indian Institute of Science, Bangalore 560012, India. E-mail: sb@iisc.ac.in

Table of Contents

1. Experimental Section	
1.1. Materials and Methods	S3
2. Chemical Synthesis and Procedures	
2.1. Synthesis	S4-S9
2.2. Procedure for dye-adsorption	S10
2.3. Procedure for estimating the quantitative dye adsorption capacity of OPN 3 and 4	S10
2.4. Procedure for <i>in situ</i> synthesis of AuNPs within OPN 4	S11
2.5. Procedure for the catalytic reduction	S11
3. Characterization	
3.1. ¹ H NMR of the precursor (Figure S1)	S12
3.2. FT-IR (Figure S2)	S13
3.3. ¹³ C NMR and ³¹ P NMR (Figure S3 and Figure S4)	S14- S15
3.4. Thermogravimetric analysis (Figure S5)	S16
3.5. TEM (Figure S6).....	S17
3.6. X-ray powder diffraction (Figure S7).....	S18
3.7. BET (Figure S8-S9, Table S1).....	S19-S20
4. Experimental results	S21-S40

1. Experimental Section

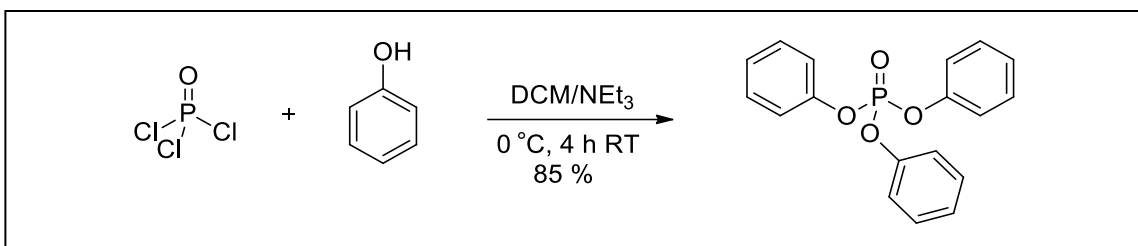
1.1. Materials and Methods. All the reagents, starting materials (quinol, 4,4'-biphenol, phloroglucinol), solvents and organic dyes were purchased from commercial suppliers and were used without further purification. Solvents were dried as per literature procedure prior to use according to the requirements. Thin layer chromatography (TLC) on silica gel GF₂₅₄ was used for the determination of R_f values, and the visualization was performed by irradiation with UV lamp at 254 nm. Column chromatography was performed on Merck silica gel (60-120 mesh) with eluent as mentioned. ¹H (500 MHz) and ¹³C (125 MHz) NMR spectra were recorded in a Bruker Ultrashield Plus-500 NMR spectrometer in deuterated solvent at ambient temperature (300 K). Chemical shifts are reported in ppm (δ) relative to tetramethylsilane (TMS) as the internal standard (CDCl₃ δ 7.26 ppm for ¹H and 77.0 ppm for ¹³C). Solid state ¹³C CPMAS NMR spectra were recorded in a Bruker Ultrashield Plus-500 NMR spectrometer. Solid state ³¹P CPMAS NMR was recorded in a Bruker Console: Avance I - 500 NMR spectrometer. Mass spectra were recorded on a XEVO G2-XS-Q-ToF (ESI) spectrometer. Fourier transform infrared spectra (FTIR, 4000-600 cm⁻¹) were performed on a Shimadzu FT-IR 8300 instrument, the wave numbers of recorded IR-signals are reported in cm⁻¹. Elemental analyses were carried out using a Perkin-Elmer Series-II, CHNO/S Analyser-2400. Thermogravimetric analyses (TGA) were performed on a SDT Q Series 600 Universal VA.2E TA instrument. The phosphate based organic polymer networks (OPNs) were observed under scanning electron microscope (SEM) model JSM 6700F JEOL Ltd. made in Japan. The samples were prepared on brass stubs by adding powder polymers mounting on top of double-sided tapes. TEM measurements were carried out in a JEOL-2010EX machine operating at an accelerating voltage of 200 V. TEM samples were prepared by mounting on the copper grid for analysis. UV-visible adsorption spectra were recorded on a Shimadzu UV-2550 UV-vis spectrophotometer. Kinetic experiment

for the dye adsorption was performed using EPOCH 2 microplate reader linked UV-vis spectrophotometer. X-ray photoelectron spectroscopy (XPS) experiment was performed using an Omicron nanotech instrument operated at 15 kV and 20 mA. X-Ray diffraction patterns of the powder organic polymer samples were obtained using a Bruker AXS D-8Advanced SWAX diffractometer using Cu-K α (0.15406 nm) radiation. The N₂ adsorption/desorption isotherms of the sample was recorded on a Micromeritics 3-Flex Surface Characterization Analyzer at 77 K.

2. Chemical Synthesis and Procedures

2.1. Synthesis

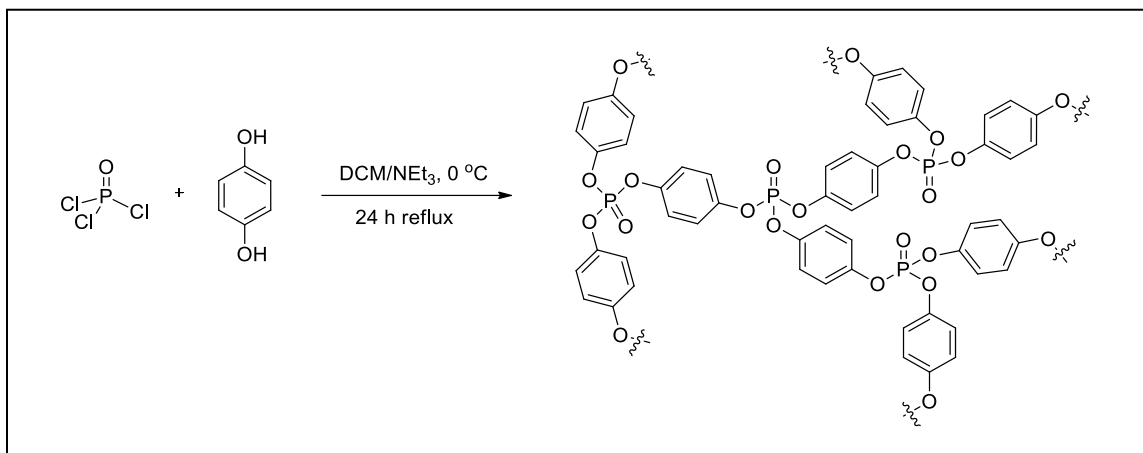
(a) Synthesis of triphenyl phosphate (model reaction):



Synthesis of the triphenyl phosphate was carried out with a modification of an existing literature procedure.^[1] Phenol (1g, 10.64 mmol) in dry dichloromethane (15 mL) was stirred in a two-necked round-bottom flask and triethyl amine (2.22 mL, 15.96 mmol) was added drop wise at 0 °C. Then, phosphoryl chloride (0.33 mL, 3.55 mmol) in 5 mL dichloromethane was slowly added to the reaction mixture at 0 °C through a dropping funnel (*the reaction was exothermic!*). The temperature was allowed to increase to room RT temperature and the reaction mixture was stirred at room temperature for additional four hours. After completion of the reaction, the reaction mixture was washed with 2N hydrochloric acid for three times, and then by distilled water for two times. Single spot was observed by thin layer chromatography and hence no further purification was performed. After solvent evaporation under vacuum, pure product was obtained as crystalline solid. Yield 85%. ¹H NMR (400 MHz, CDCl₃): 6.73 (d, 6H), 7.09-7.11

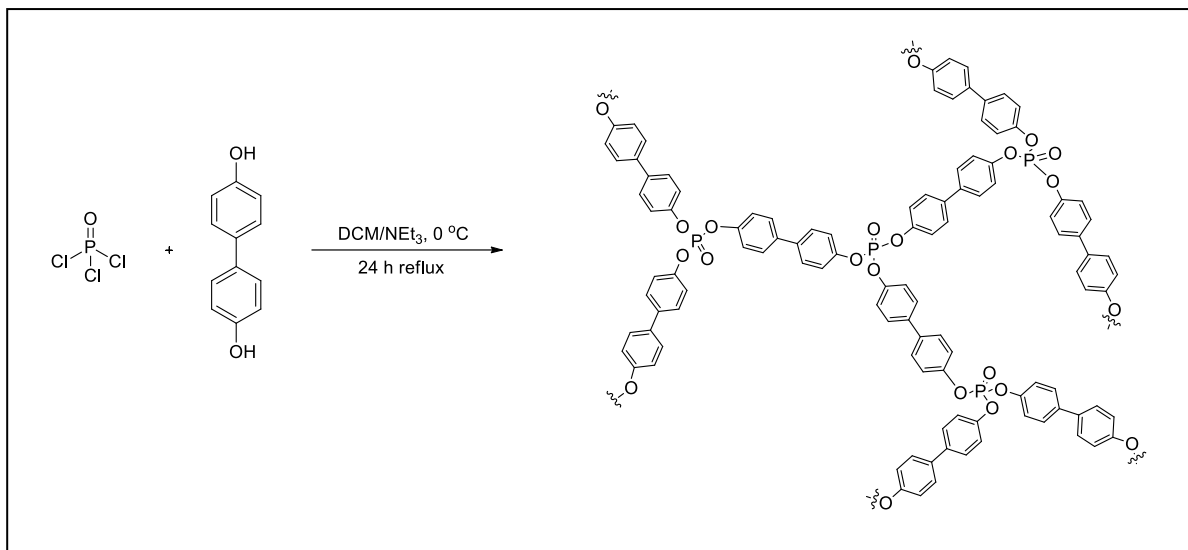
(m, 6H) 6.82-6.93 (m, 3H) ppm. ^{13}C NMR (100 MHz, CDCl_3): 120.0, 125.5, 130.0, 151 ppm. ^{31}P NMR (162 MHz, CDCl_3): -17.70 ppm.

(b) Synthesis of OPN 1:



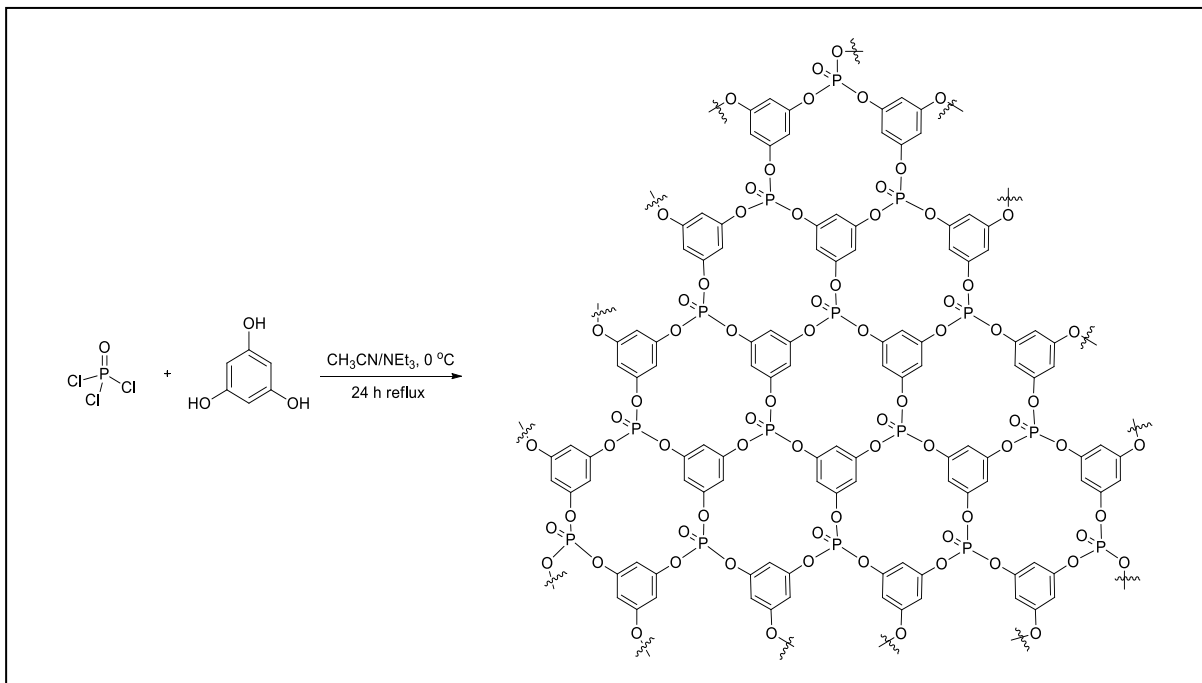
In a two-neck round-bottom flask, quinol (2 g, 18.18 mmol) in dry dichloromethane (30 mL) was stirred and triethylamine (4.599 g, 45.45 mmol) was added dropwise at ice-cold condition. Then, phosphoryl chloride (1.85 g, 12.12 mmol) in 10 mL dry dichloromethane was added dropwise to the reaction mixture at 0 °C through a dropping funnel. The temperature was allowed to increase to room temperature and the reaction mixture was gently refluxed for 24 h. After completion of the reaction, 2N hydrochloric acid was added to neutralize the excess triethylamine followed by filtration and washing with distilled water and methanol. The product was washed in Soxhlet apparatus with methanol and chloroform (1 day for each solvent) and dried under vacuum at 80 °C to obtain OPN 1 as white hygroscopic solid (Yield 96%). FTIR: 3438, 1500, 1162, 955, 825 cm^{-1} . ^{13}C CPMAS NMR: 100-160 ppm. Elemental analysis calculated for $\text{C}_{18}\text{H}_{12}\text{O}_8\text{P}_2$ (considering trapped $3\text{H}_2\text{O}$): C, 45.78; H, 3.84; found: C, 46.04; H, 3.32. TGA under N_2 : 5% weight loss at 195 °C.

(c) Synthesis of OPN 2:



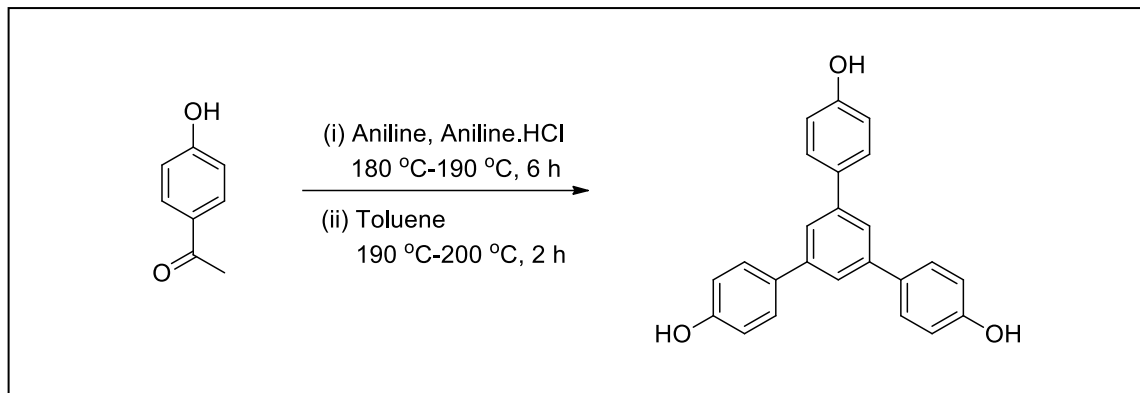
4,4'-Biphenol (2 g, 10.7 mmol) was dissolved in 40 mL dry dichloromethane and dry triethylamine (3.75 mL, 26.85 mmol) was added to it slowly at ice-cold condition. Then, phosphoryl chloride (1.103 g, 7.196 mmol) in 10 mL dichloromethane was added dropwise at 0 °C over a period of 30 min through a dropping funnel. The reaction temperature was allowed to increase to room temperature and then the mixture was gently refluxed for 24 h. After completion of the reaction, 2N hydrochloric acid was added to neutralize the excess triethylamine followed by filtration and washing with distilled water and methanol. The product was washed in Soxhlet apparatus with methanol and chloroform (1 day for each solvent) and dried under vacuum at 80 °C to obtain OPN 2 as white solid (Yield 92%). FTIR: 3424, 1619, 1183, 1041, 939 cm⁻¹. ¹³C CPMAS NMR: 100-160 ppm. Elemental analysis calculated for C₃₆H₂₄O₈P₂ (considering trapped 3H₂O): C, 61.72; H, 4.32; found: C, 61.29; H, 4.02. TGA under N₂: 5% weight loss at 375 °C.

(d) Synthesis of OPN 3:



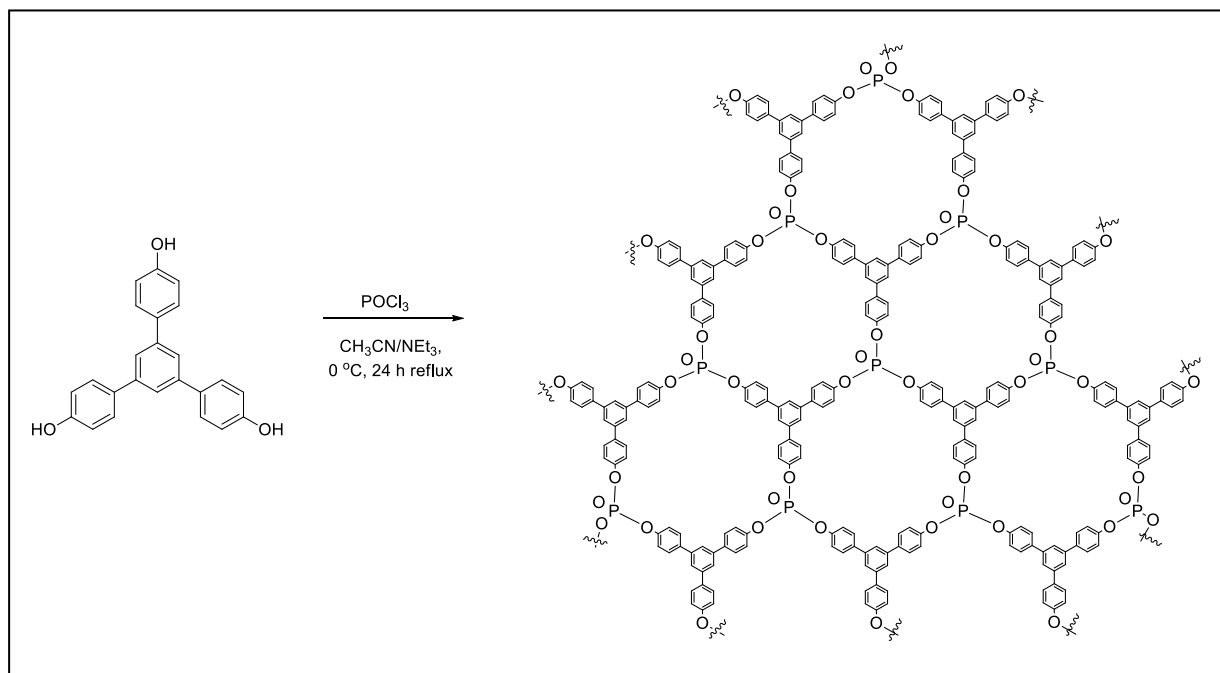
Anhydrous phloroglucinol (1.55 g, 12.43 mmol) was taken with 20 mL dry acetonitrile in a round-bottom flask and dry triethylamine (6.2 mL, 44.42 mmol) was added slowly to the reaction mixture at ice-cold condition. Phosphoryl chloride (1.5 mL, 12.34 mmol) in 10 mL dry acetonitrile was added dropwise through a dropping funnel over a period of 30 min. Thereafter, the reaction mixture was warmed to room temperature and then gently refluxed for 24 hours. After completion of the reaction, 2N hydrochloric acid was added to neutralize the excess triethylamine followed by filtration and washing with distilled water and methanol. The product was washed in Soxhlet apparatus with methanol and chloroform (1 day for each solvent) and dried under vacuum at $80\text{ }^\circ\text{C}$ to obtain OPN 3 as white solid (Yield 93%). FTIR: 3424, 1619, 1269, 1128, 1027 cm^{-1} . ^{13}C CPMAS NMR: 100-160 ppm. Elemental analysis calculated for $\text{C}_6\text{H}_3\text{O}_4\text{P}$ (considering trapped $2\text{H}_2\text{O}$): C, 34.97; H, 3.42; found: C, 35.06; H, 4.05. TGA under N_2 : 5% weight loss at $160\text{ }^\circ\text{C}$.

(e) Synthesis of 1,3,5-(4-hydroxyphenyl)benzene:



4-Hydroxyacetophenone (6.8 g, 50 mmol) was stirred with aniline (9.3 g, 100 mmol) and aniline hydrochloride (0.25 g, 1.93 mmol) at a refluxing temperature of 185-190 °C for 4 h. After this period, 6 mL of toluene was added to the reaction mixture and further refluxed at 190-200 °C for another 2 h. Then, heating was continued and most of the aniline was distilled out from the reaction mixture. The residue was poured into 2N hydrochloric acid and extracted with ethyl acetate. The organic layer was thoroughly washed with water. The product was purified by silica gel column chromatography eluting with 30% ethyl acetate in petroleum ether to obtain pure product as white solid (Yield 82%). ¹H NMR (400 MHz, CDCl₃): 7.66 (s, 3H), 7.31-7.42 (d, 6H), 6.79-6.83 (d, 6H), 5 (s, 1H) ppm. ¹³C NMR (100 MHz, CDCl₃): 156.2, 137.6, 129.2, 128.8, 125.2, 116.2 ppm.

(f) Synthesis of OPN 4:



1,3,5-(4-Hydroxyphenyl)benzene (500 mg, 1.412 mmol) was stirred with 20 mL dry acetonitrile and 0.7 mL dry triethylamine was added slowly at ice-cold condition. Then phosphoryl chloride (216.5 mg, 1.412 mmol) dissolved in 5 mL dry acetonitrile was added dropwise through a dropping funnel over a period of 30 min at 0 °C. The reaction mixture was warmed to room temperature followed by gentle refluxing for 24 h. After completion of the reaction, 2N hydrochloric acid was added to neutralize the excess triethylamine followed by filtration and washing with distilled water and methanol. The product was washed in Soxhlet apparatus with methanol and chloroform (1 day for each solvent) and dried under vacuum at 80 °C to obtain OPN 4 as yellowish-white solid (Yield 77.8%). FTIR: 3398, 1603, 1157, 977, 837 cm^{-1} . ^{13}C CPMAS NMR: 100-160 ppm. Elemental analysis calculated for $\text{C}_{24}\text{H}_{15}\text{O}_4\text{P}$ (considering trapped 1.75 H_2O): C, 66.36; H, 4.41; found: C, 66.65; H, 5.05. TGA under N_2 : 5% weight loss at 260 °C.

2.2. Procedure for dye-adsorption:

In four separate vials, 1 mg each of the OPNs **1-4** was weighed and added into a solution of methylene blue (20 μM) in ethanol. This mixture in each vial was stirred at room temperature for 1 h at first. Thereafter the vials were either allowed to stand undisturbed overnight for the precipitates to settle down or the mixtures were centrifuged at 6000 rpm to separate the adsorbed dye within the OPNs from the bulk. In both the methods, the unabsorbed dye in the solution was taken for recording the UV-vis spectra. The spectra so obtained for each of the four solutions was compared to that of the dye alone in ethanol (20 μM) to compare the extent of dye adsorption among OPNs **1-4**.

2.3. Procedure for estimating the quantitative dye adsorption capacity of OPN 3 and 4:

In separate vials, 1 mg each of the OPN **3** and **4** were weighed and added into 1 mL of ethanol solution. A 2 mM methylene blue stock solution in ethanol was prepared in another vial. From there, 5 μL of the methylene blue solution was taken accurately using a micropipette and added to each vial containing the OPN **3** and **4**. Both the mixtures were stirred at room temperature until the dye was completely adsorbed by OPN **3** and **4**. Following that, another 5 μL of the methylene blue dye solution was added to each vial again and the stirring was continued until the dye was completely adsorbed as discerned from naked eye. This process was repeated for several times until the extent of dye adsorption finally reached a saturation in both the cases and the residual dye remained in the solution as confirmed from its blue color. The quantitative dye adsorption capacity was calculated to be 39 ± 5 mM/g for OPN **3** and 275 ± 5 mM/g for OPN **4**. This confirmed that OPN **4** was a better candidate for the dye adsorption compared to OPN **3**.

2.4. Procedure for *in situ* synthesis of AuNPs within OPN 4:

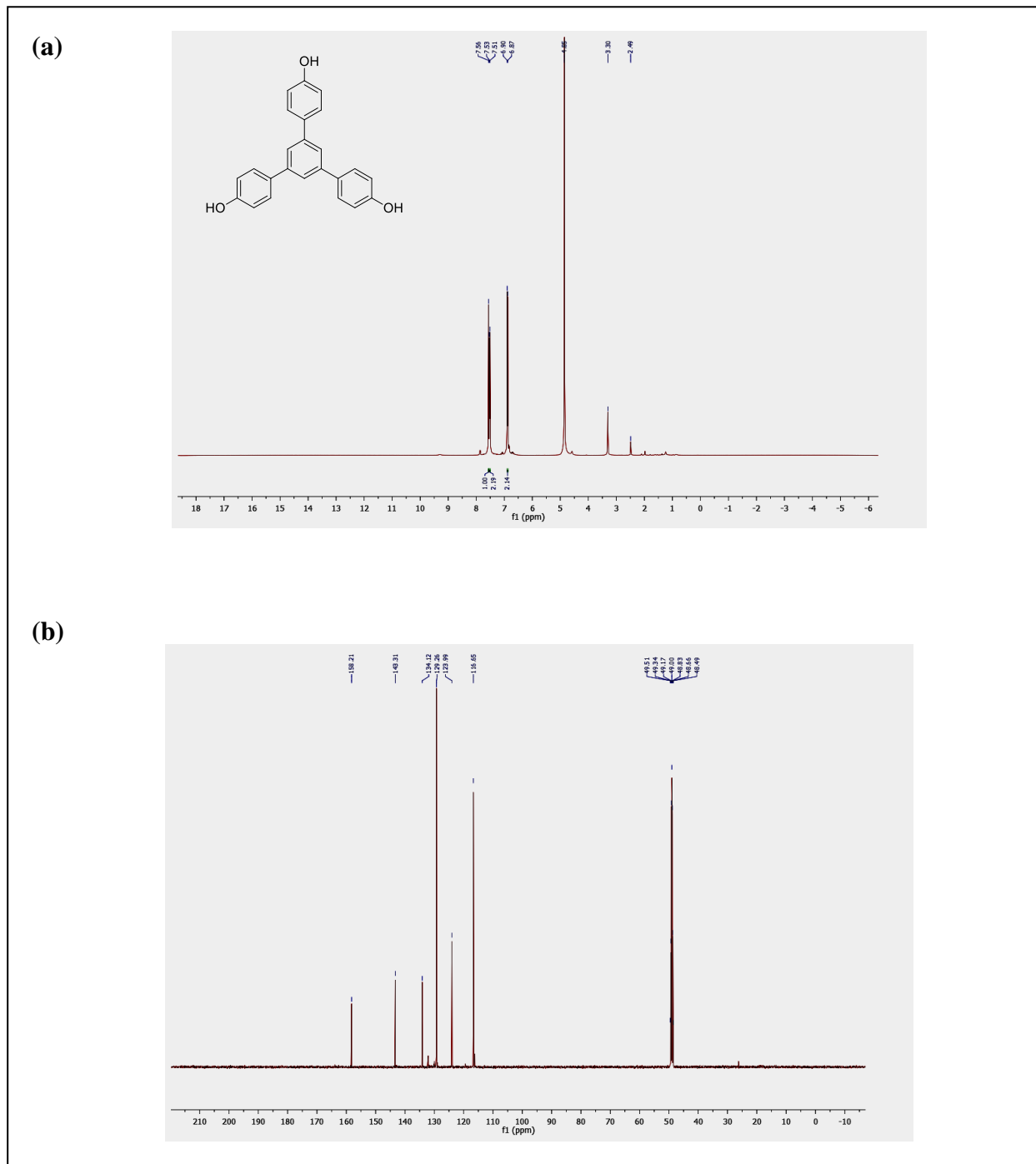
In a vial, a 2 mL solution of HAuCl₄ (1 mM) and 1 mg of the OPN 4 were mixed and then boiled with gentle stirring for 10 min. Following that, 1 mL of trisodium citrate (34 mM) solution was added dropwise into the reaction mixture and the mixture was continued boiling for another 30 min. The solution soon turned wine red indicating the formation of stable suspension of gold nanoparticles (AuNPs) loaded OPN 4. The mixture was centrifuged at 6000 rpm and the residue was washed several times with deionized water and dried under vacuum to obtain the solid AuNP loaded OPN 4 powder.

2.5. Procedure for the catalytic reduction:

In a typical experiment, a 200 μL of aqueous solution of 1.4×10^{-4} M, 4-nitrophenol was prepared in a vial and was mixed with 800 μL of aqueous solution of 0.1 M NaBH₄. Thereafter, 1 mg of AuNP loaded OPN 4 was added into the reaction mixture and stirred at room temperature. The solution turned colorless (due to the formation of 4-aminophenol) from lemon yellow (due to 4-nitrophenol) over a period of 30 min, ensuring completion of the reduction process. However, when the same step was performed with empty OPN 4 no such change in color was observed. This observation was further confirmed by recording UV-vis absorption spectra of the corresponding solutions and ¹H NMR of the isolated products in each case.

3. Characterizations

3.1. ^1H NMR of the precursor



3.2. FT-IR

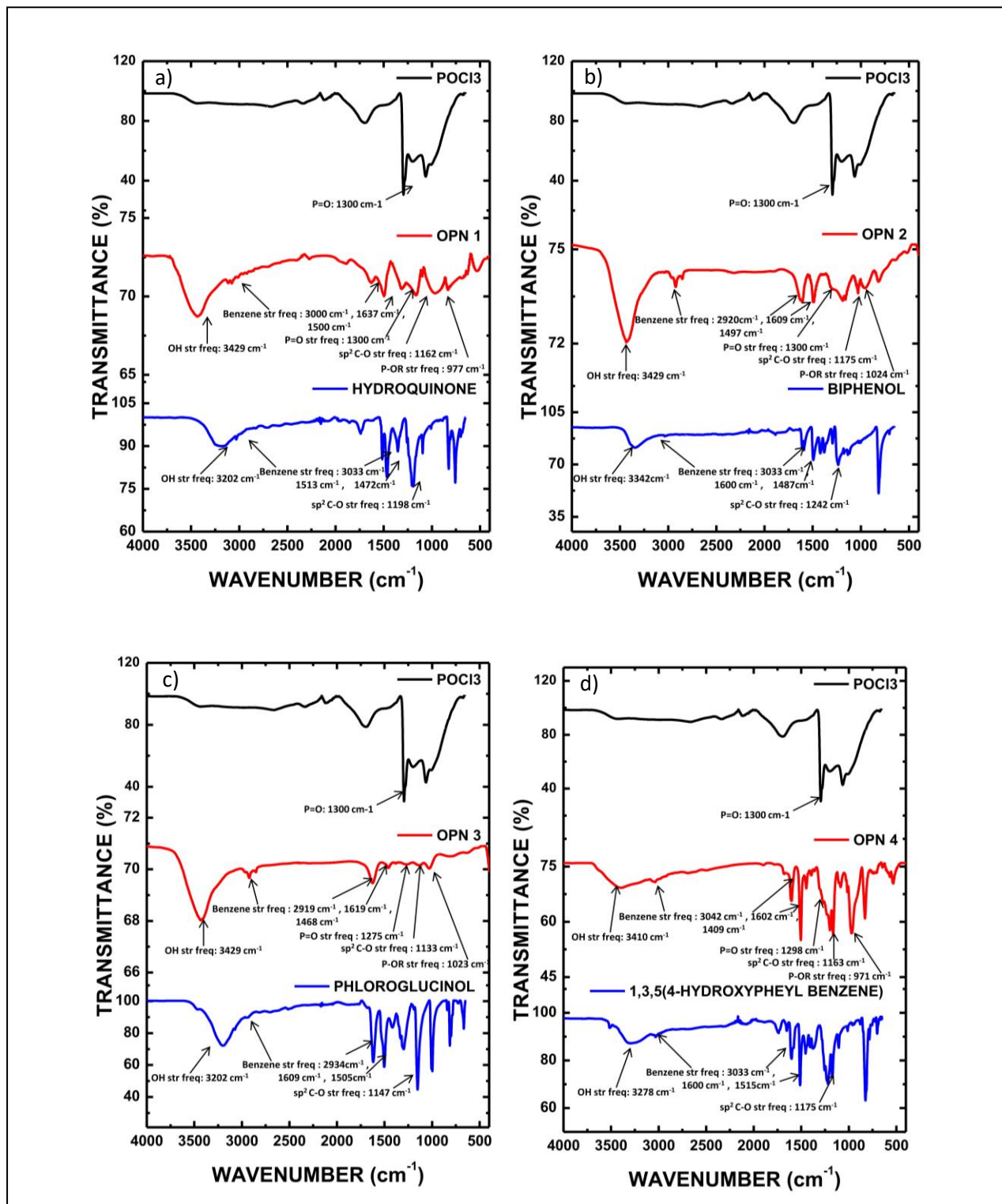


Figure S2. FTIR spectra (KBr pellets) of the OPNs (a) 1, (b) 2, (c) 3 and (d) 4.

3.3. ^{13}C NMR and ^{31}P NMR

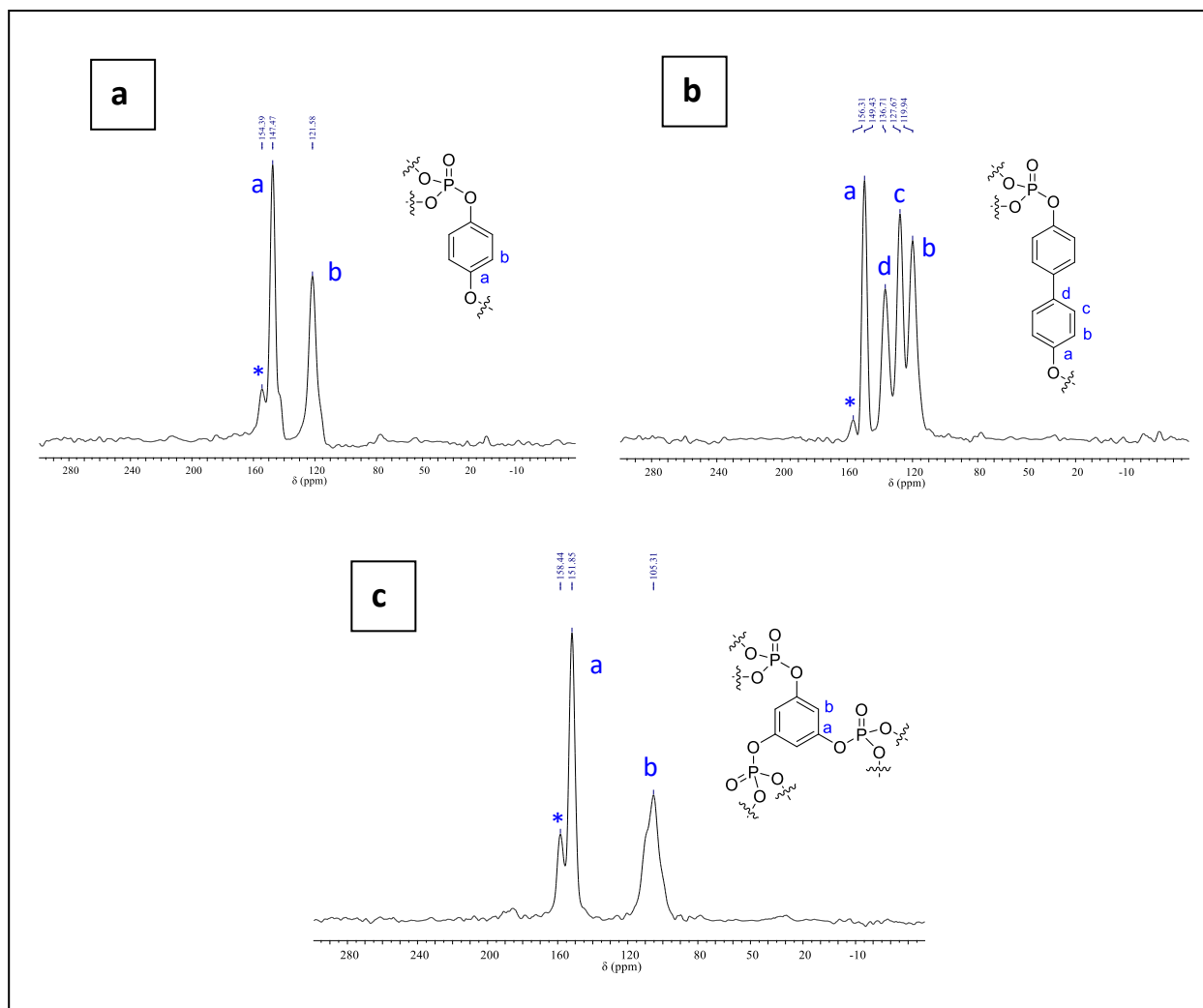


Figure S3. ^{13}C CPMAS NMR of the OPNs (a) **1**, (b) **2**, and (c) **3**. Peaks assigned by (*) are possibly due to the end groups.

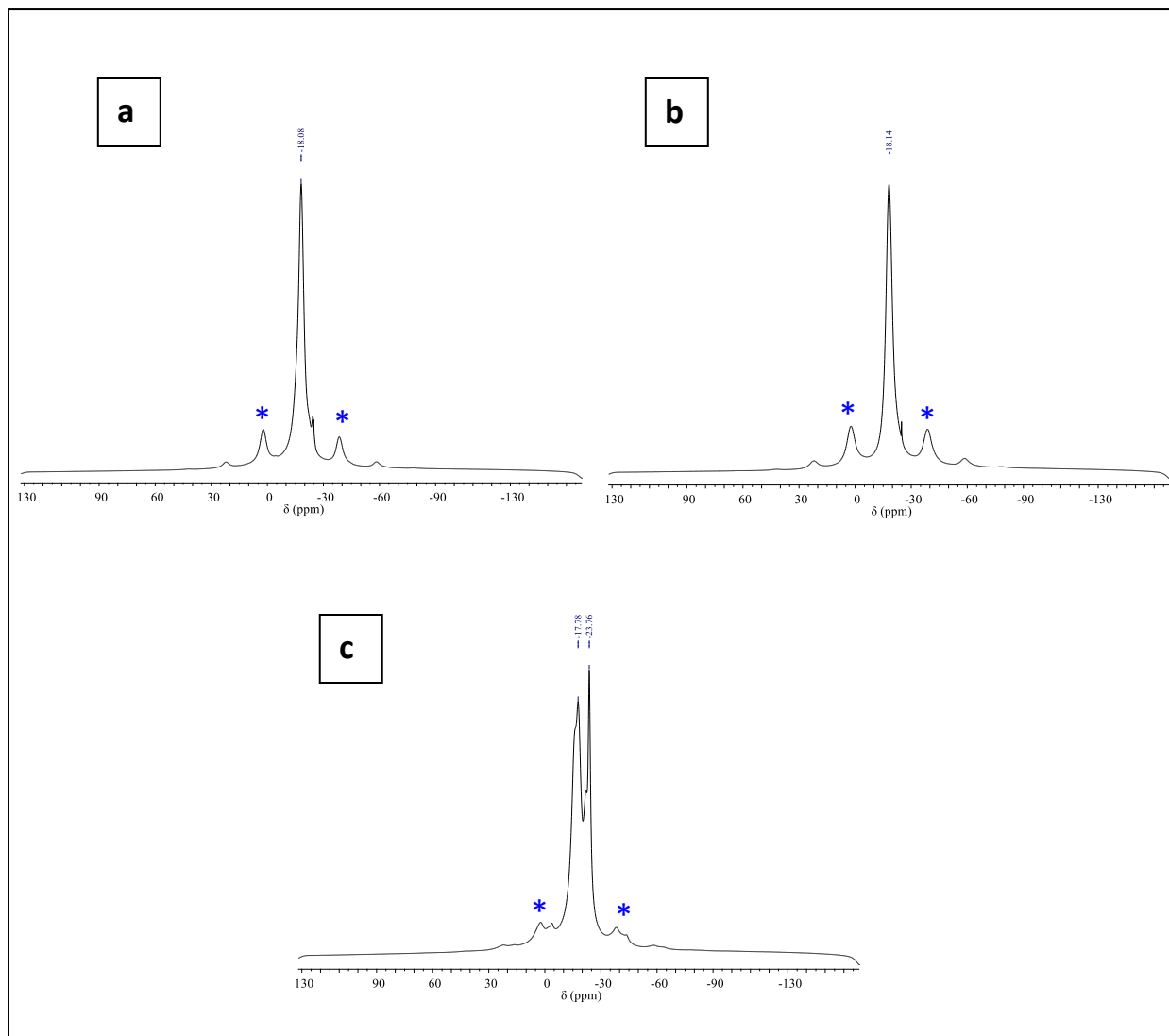


Figure S4. ^{31}P NMR of the OPNs (a) **1**, (b) **2**, and (c) **3**. Two peaks in case of OPN **3** could be due to the end phosphate groups where two of the -OH groups of the end phloroglucinol moieties are present in the tautomeric 'keto' form. Peaks assigned by (*) are due to the spinning sidebands.

3.4. Thermogravimetric analysis

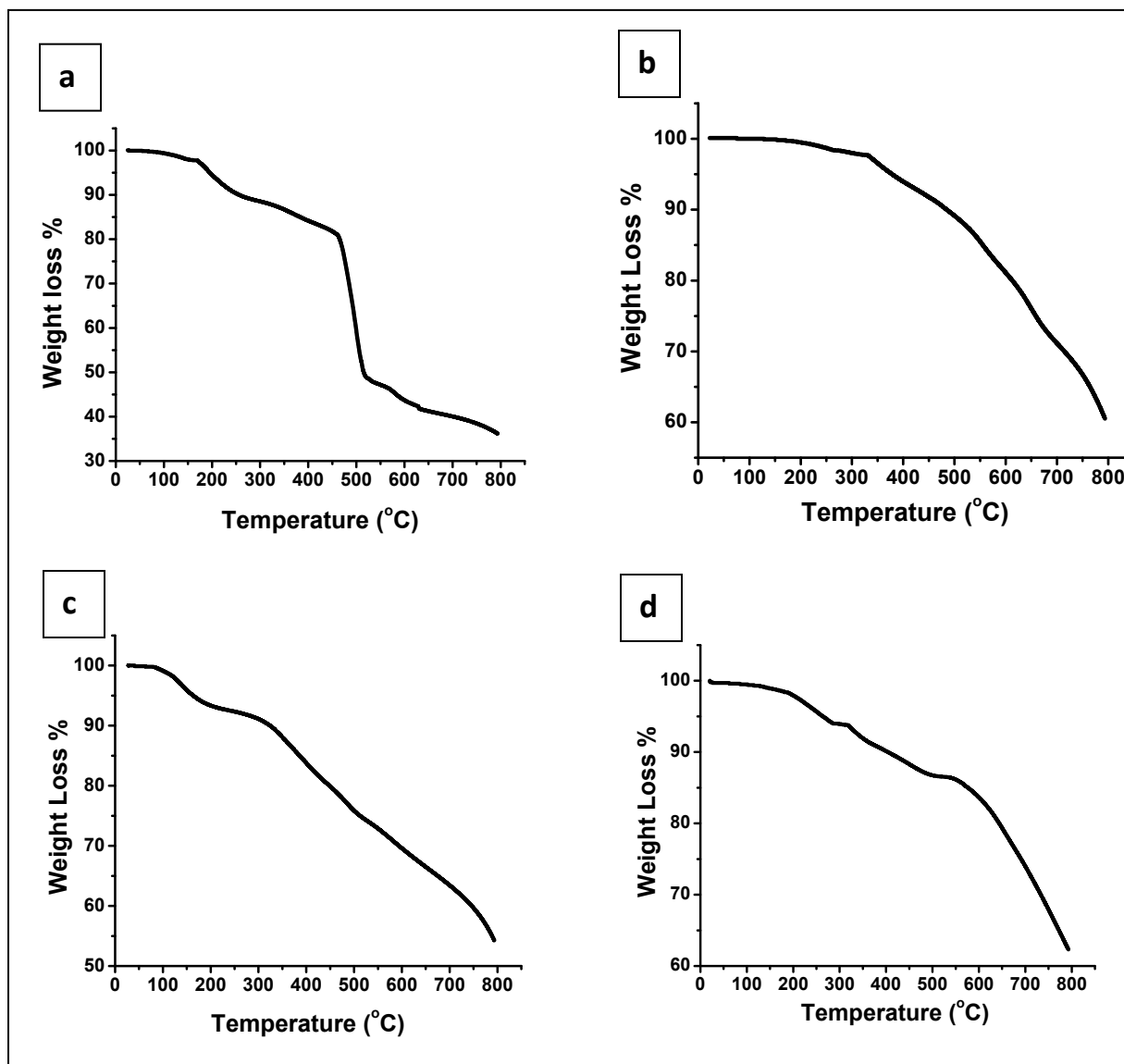


Figure S5. TGA curves of the OPNs (a) **1**, (b) **2**, (c) **3** and (d) **4**. The degradation temperatures at 5% weight loss were found to be at 195 °C, 375 °C, 160 °C and 260 °C for the OPNs **1-4** respectively. It is evident from the TGA results that the presence of lesser phosphate groups make the network more thermally stable. Thus, OPN**1** and OPN**2** showed greater thermal stability as compared to OPN**3** and OPN**4**, respectively. For a larger aromatic linker, thermal stability increases, as expected. Thus, OPN**2** and OPN**4** are thermally more stable than OPN**1** and OPN**3** respectively.

3.5. TEM

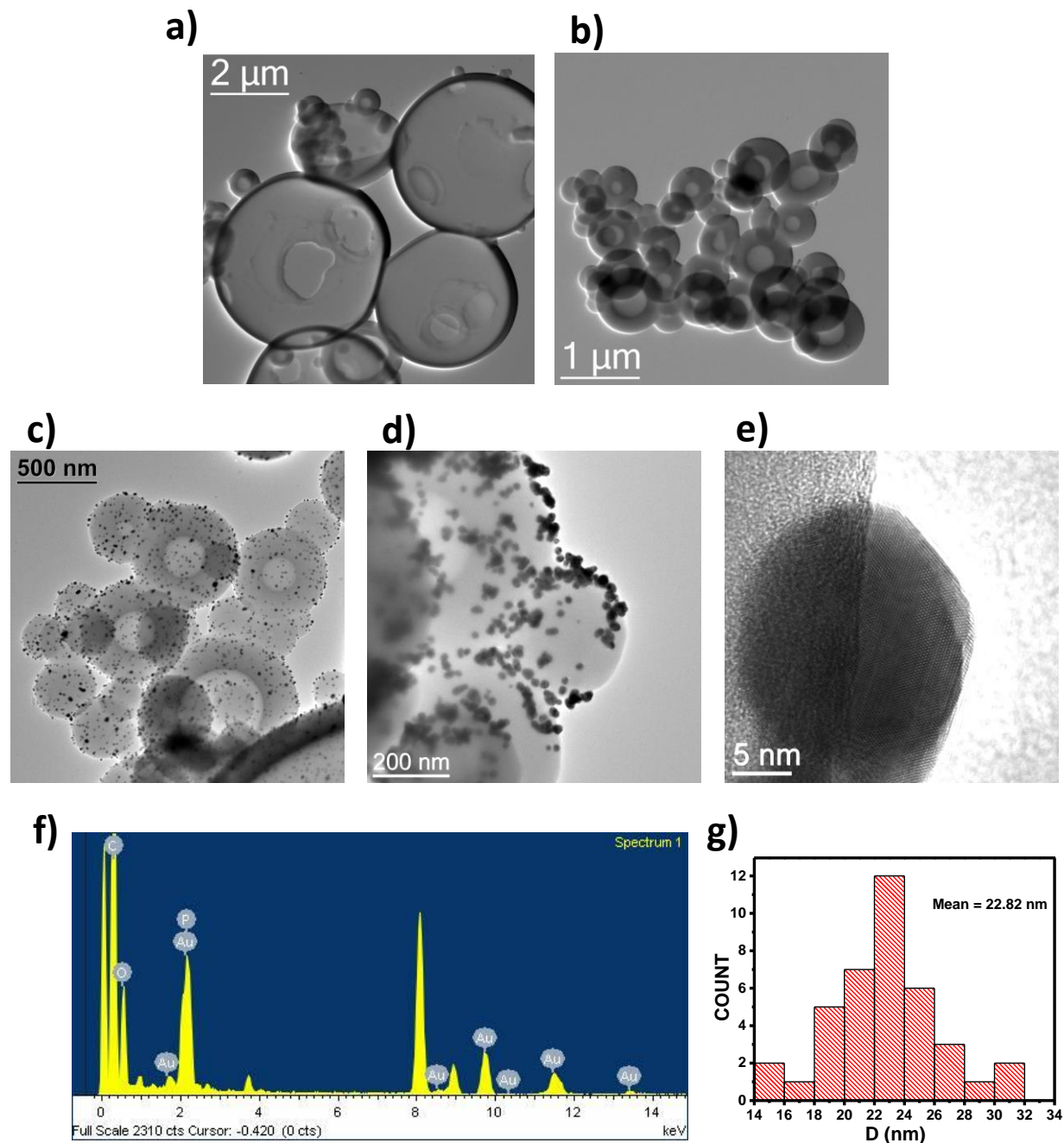


Figure S6. TEM images of (a, b) OPN 4 showing hollow spheres of two kinds. The bigger spheres have diameter ranging from 2-4 μm with one or more openings. However, the smaller spheres have diameter typically less than 1 μm with no visible openings. From TEM (as well as SEM) images, it was observed that the bigger spheres contribute significantly more than the smaller spheres in its morphology. (c, d) TEM images of AuNPs loaded OPN 4 and (e) crystal fringes of AuNPs in AuNPs loaded OPN 4. (f) EDX data of the AuNPs loaded OPN 4 and (g) size distribution of the AuNPs loaded OPN 4.

3.6. X-ray powder diffraction (XRD)

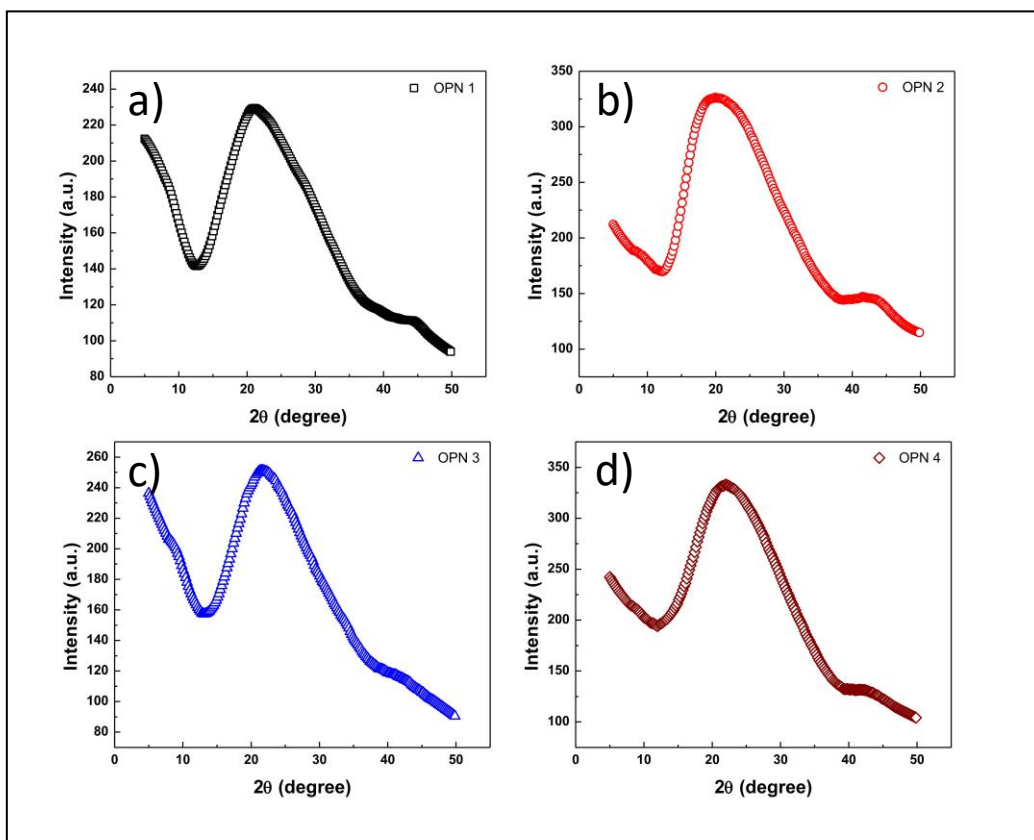


Figure S7. Powder X-ray diffraction pattern of the OPNs (a) 1, (b) 2, (c) 3 and (d) 4.

3.7. N₂ sorption studies for BET surface area calculation

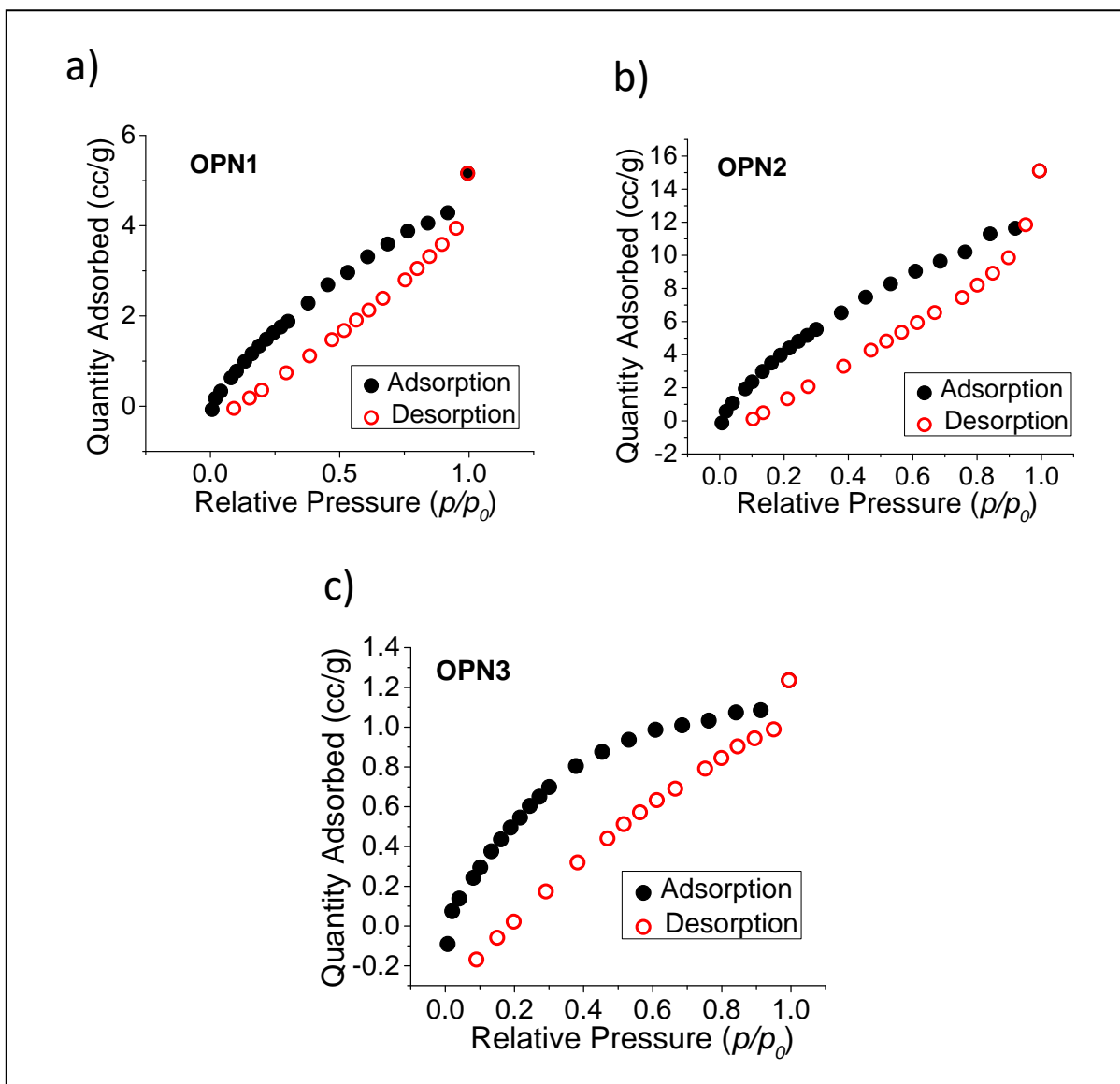


Figure S8. Nitrogen adsorption-desorption studies at 77 K for BET surface area calculation of the OPNs (a) 1, (b) 2, and (c) 3. The calculated BET surface area values are 9 m²/g (OPN 1), 25 m²/g (OPN 2), and 3 m²/g (OPN 3). The low surface area of the OPNs were probably due to the flexible nature of the phosphate-based network structures.

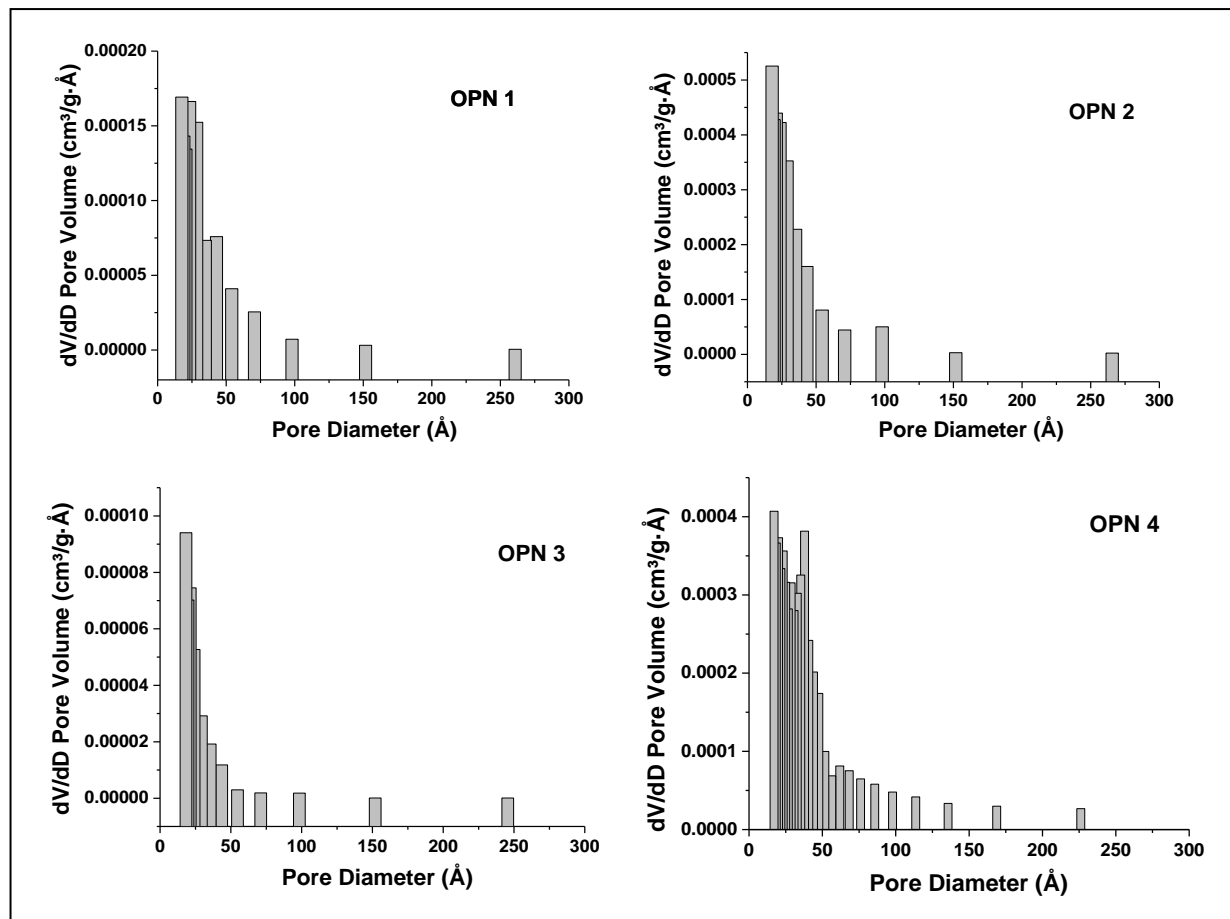


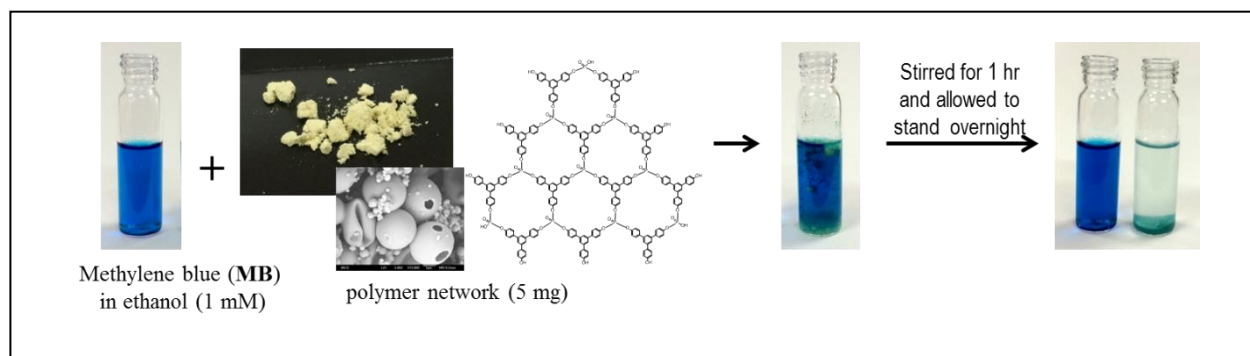
Figure S9. Pore size distribution for OPN 1-4. The analysis clearly shows that while OPN 1-3 show largely micropores, OPN 4 has micropore along with sufficient amount of mesopores.

Table S1. Summary of BET surface area, pore size distribution and the dye adsorption data and the particle diameter from SEM images for OPN 1-4. These data indicate that the dye adsorption took place in the surface of the polymers by electrostatic interactions rather than in the pores.

	OPN 1	OPN 2	OPN 3	OPN 4
BET Surface area (m ² /g)	9	25	3	20
Pore Volume (BJH, cm ³ /g)	0.00707	0.02044	0.00148	0.04164
Pore diameter (BJH, nm)	4.3	4.8	3.4	7.8
Amount of MB adsorbed (mM/g)	9	14	39	275
Particle diameter (SEM, nm)	~50	~200	~450	~3000


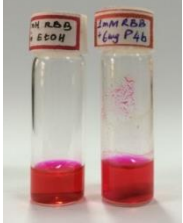

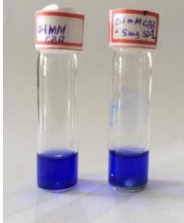

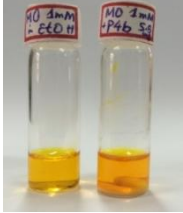

4. Experimental Results

Dye Adsorption Studies



Scheme S1. Schematic depiction of a typical dye adsorption experiment. Addition of the OPNs into a dye solution led to the dye adsorption upon stirring at room temperature. After settling for overnight, the insoluble OPNs with adsorbed dyes precipitated leaving a clear supernatant which is clearly distinct from the solution containing dye alone.

Table S2. Selectivity of OPN **4** in adsorbing cationic, anionic, neutral and zwitterionic dyes.

CATIONIC DYES	ANIONIC DYES	NEUTRAL DYES	ZWITTERIONIC DYES
<p>Methylene blue</p>  <chem>CN(C)c1ccc2nc3ccc(N(C)C)cc3s2c1Cl</chem> <p>RESULT- SHOWED STRONG ADSORPTION</p>	<p>Rose bengal base</p>  <chem>ClC1=C(Cl)C(Cl)=C(ONa)C(=O)C1=O</chem> <p>RESULT- NO ADSORPTION</p>	<p>Calcein</p>  <chem>OC(=O)CN(C)Cc1ccc(O)c2c3c(O)c(O)cc(O)cc3c(O)c2c1</chem> <p>RESULT- NO ADSORPTION</p>	<p>Coomassie brilliant blue</p>  <chem>CCN(C)Cc1ccc(S(=O)(=O)O)cc1</chem> <p>RESULT- NO ADSORPTION</p>
<p>Propidium iodide</p>  <chem>CN(C)CCN(C)C.[I-]</chem> <p>RESULT- SHOWED ADSORPTION</p>	<p>Methyl Orange</p>  <chem>CN(C)Cc1ccc(Nc2ccc(S(=O)(=O)O)cc2)cc1</chem> <p>RESULT- NO ADSORPTION</p>		
<p>Rhodamine 6 G</p>  <chem>CCN(C)C.[Cl-]</chem> <p>RESULT- SHOWED LITTLE ADSORPTION</p>			

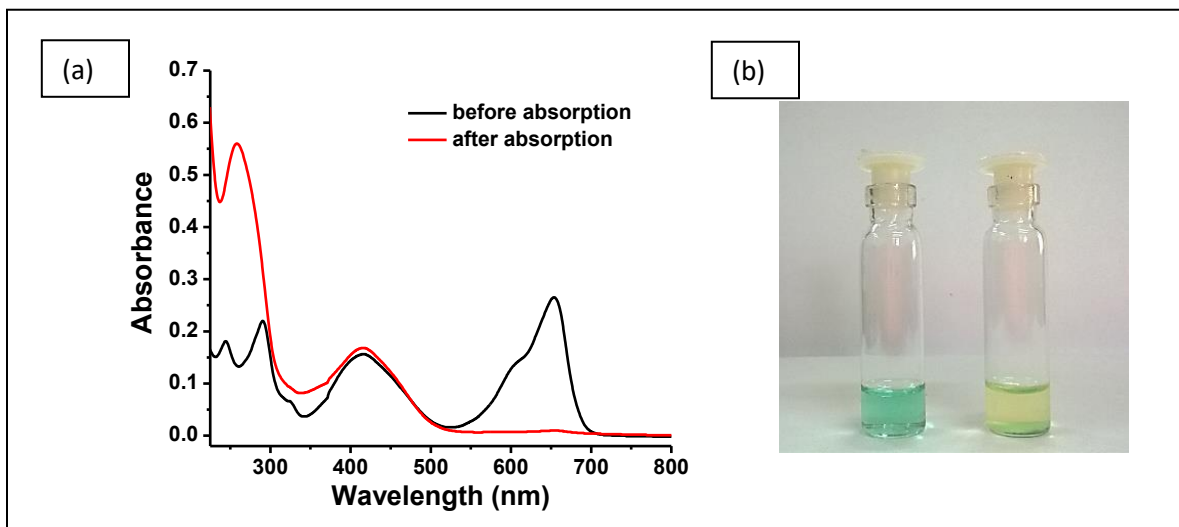


Figure S10. (a) UV-vis spectra showing selective adsorption of methylene blue by OPN **4** from a mixture of methylene blue and methyl orange and (b) vials showing corresponding solutions: left vial contains mixture of both the dyes in ethanol (conc. 20 μ M for each dye) and right vial additionally contains OPN **4** (1 mg).

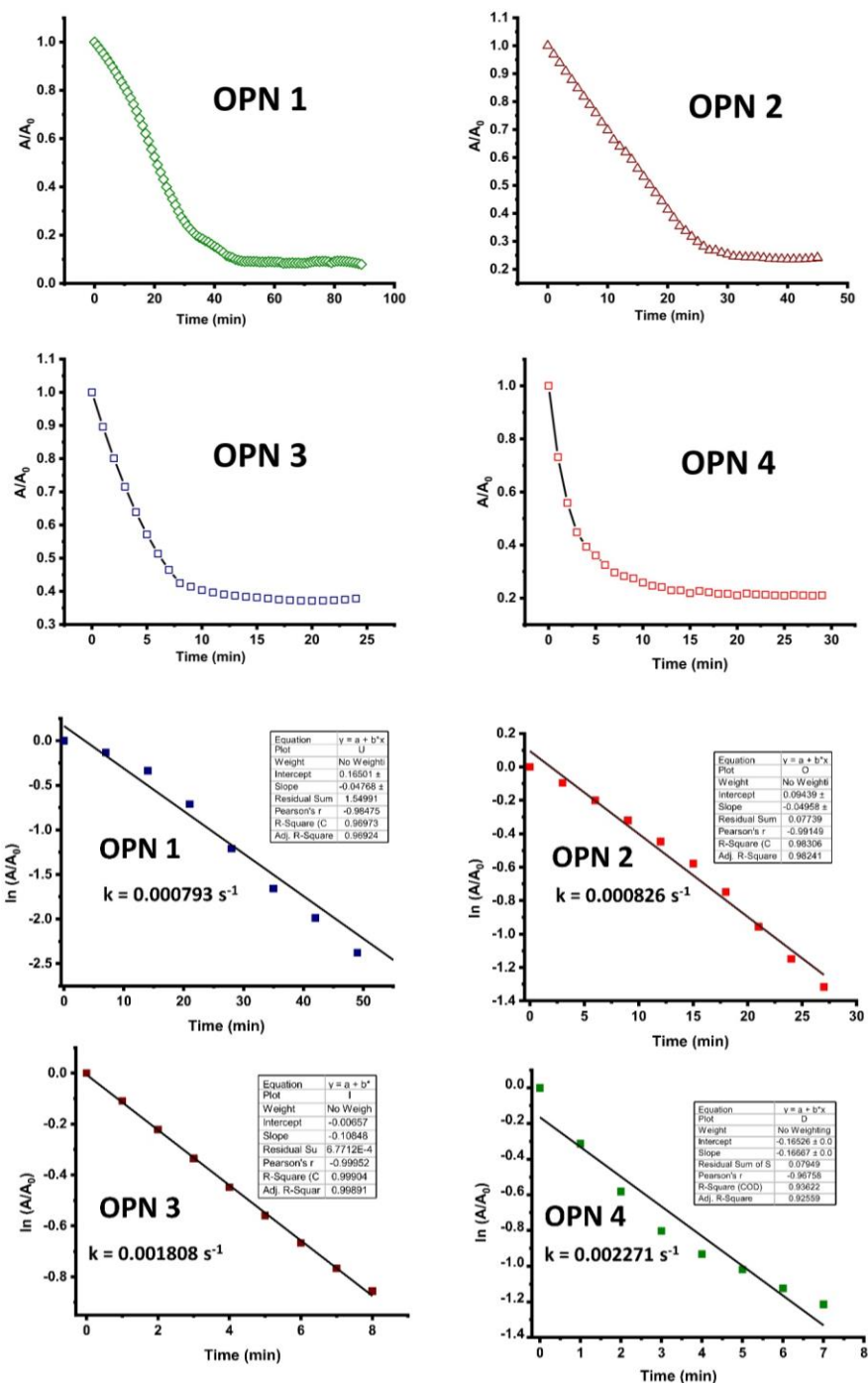


Figure S11. Kinetics of methylene blue dye adsorption by OPN 1-4 probed at 655 nm wavelength. To a 200 μ L of methylene blue solution in ethanol (20 μ M), 0.1 mg each of the OPNs were added. The spectra revealed that the dye adsorption phenomenon followed an apparent pseudo-first-order kinetics. The rate constants of the dye adsorption were calculated from the slope of the plot $\ln(A/A_0)$ vs time and were estimated to be $7.93 \times 10^{-4} \text{ s}^{-1}$, $8.26 \times 10^{-4} \text{ s}^{-1}$, $1.8 \times 10^{-3} \text{ s}^{-1}$ and $2.27 \times 10^{-3} \text{ s}^{-1}$ for OPN 1, OPN 2, OPN 3 and OPN 4 respectively. Therefore, the dye adsorption is fastest for the OPN 4.

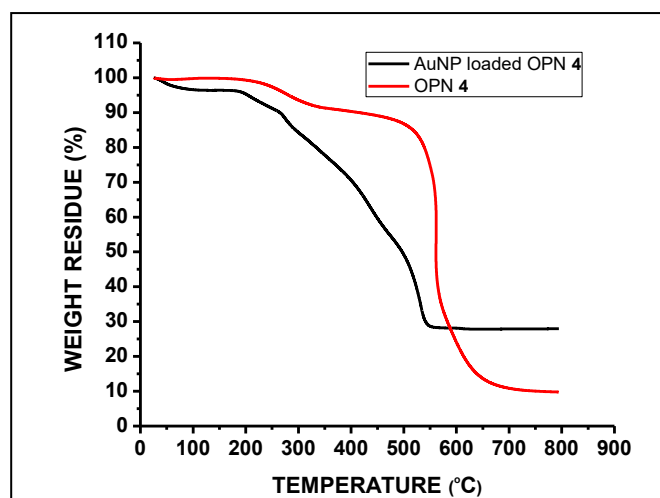


Figure S12. TGA curves of the OPN **4** and AuNP loaded OPN **4** under ambient condition. The TGA experiment was performed to determine the amount of AuNPs present within the OPN **4**. The analysis was performed under a flow of 100 mL/min air while the change in mass was determined every 0.1 °C over a temperature range of 25–800 °C. The amount of residue remaining for the OPN **4** was 9.66 % and that for AuNP loaded OPN **4** was 28.3%. Accordingly, 18.64 % of AuNPs was present within the OPN **4**. This experiment was performed with 4.413 mg of AuNP loaded OPN **4**, so 0.8225 mg of AuNP was present in it. Therefore, 1 mg of OPN **4** was loaded with 0.1864 mg of AuNPs, leading to a molar concentration of AuNPs in OPN **4** as 0.95 mM.

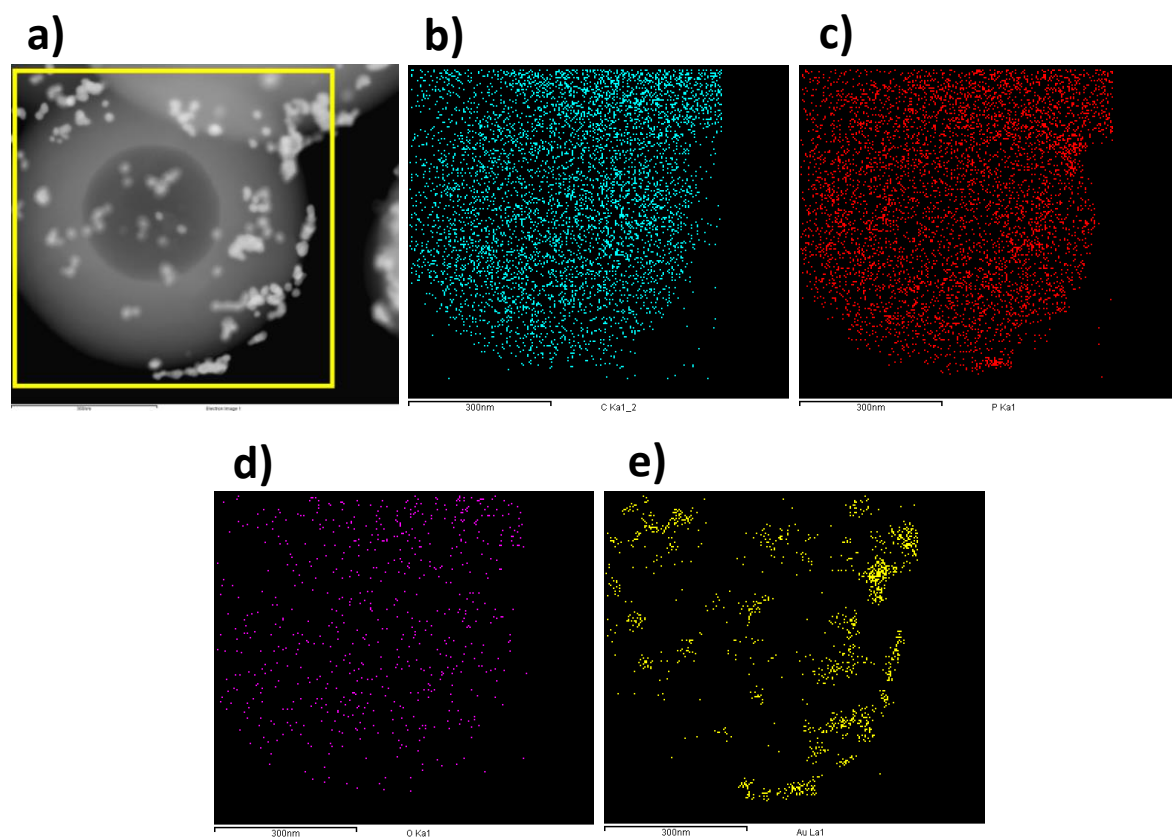


Figure S13. High-angle annular dark-field (HAADF) TEM images showing elemental mapping figures for the (a) selected area of AuNP loaded OPN **4**, (b) element C, (c) element P, (d) element O and (e) element Au. These images showing homogeneous distribution of the elements in the sample.

X-ray photoelectron spectroscopy

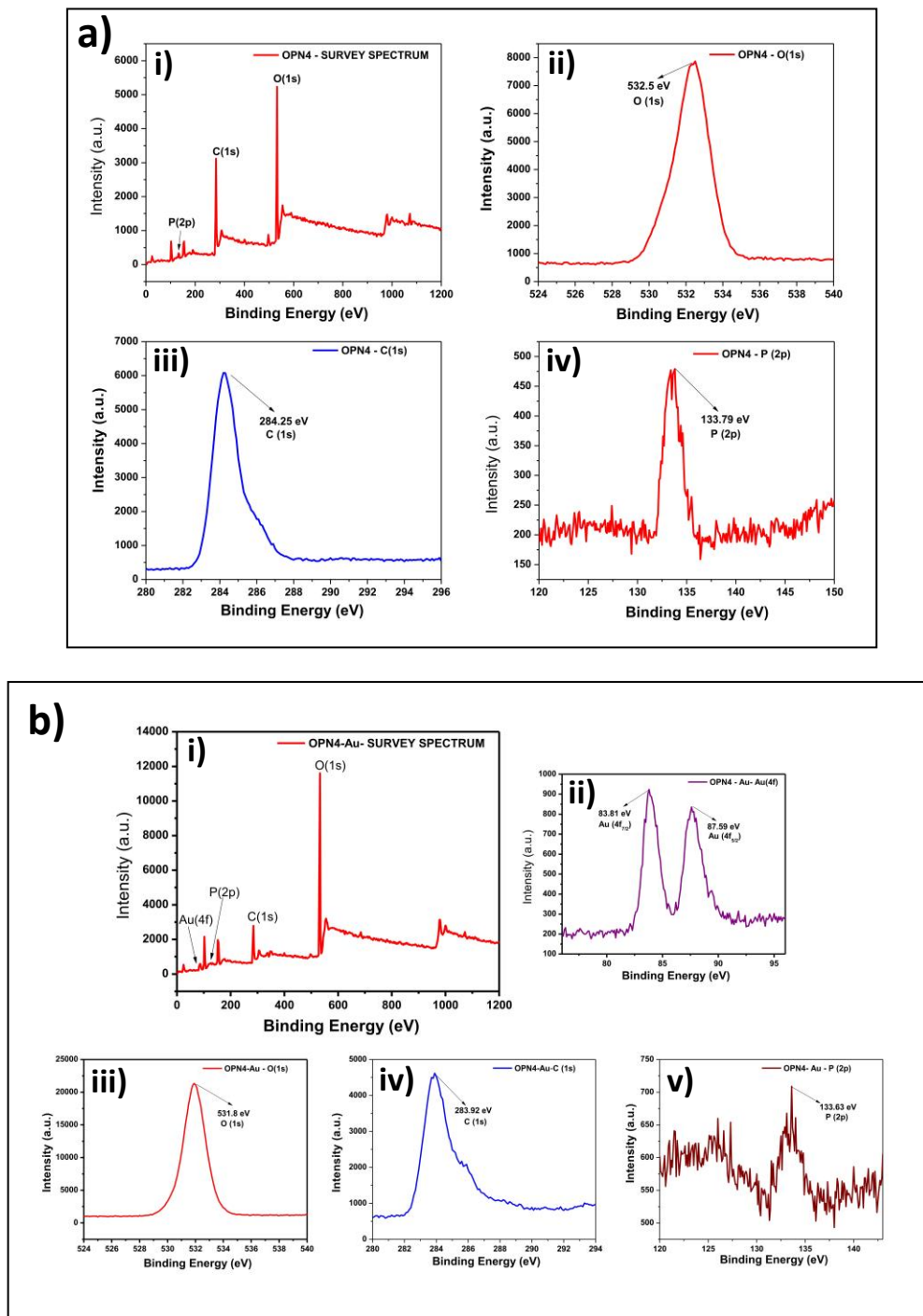


Figure S14. X-ray photoelectron spectroscopy data of (a) OPN 4 [(i) survey XPS spectrum and high-resolution spectra of (ii) O 1s, (iii) C 1s and (iv) P 2p of OPN 4] and (b) OPN 4-Au [(i) survey XPS spectrum of OPN 4-Au and high-resolution spectra of (ii) Au 4f, (iii) O 1s, (iv) C 2s and (v) P 2p of OPN 4-Au. The elements in the OPN4 were analyzed by the deconvolution of the

peaks obtained from the spectra of the XPS measurements. The C(1s) peak at $\sim 284.25\text{eV}$ indicated the presence of sp^2 carbons of the aromatic moieties in the OPN **4**. The P(2p) peak at $\sim 133.79\text{eV}$ indicated the presence of the phosphate groups (P=O). In the O (1s) spectrum of the OPN**4**, the peak at $\sim 532.5\text{eV}$ indicated the presence of oxygen in the ester linkages. The elements in the OPN**4**-Au were also analyzed. The peaks for C(1s), P(2p) and O(1s) were obtained at 283.92eV , 133.63eV and 531.8eV respectively. These peaks corresponded to the polymer framework. The AuNPs embedded on the surface of the OPN**4** was confirmed from the peaks obtained at 83.81eV and 87.59eV for the Au(4f $_{7/2}$) and Au(4f $_{5/2}$) respectively.

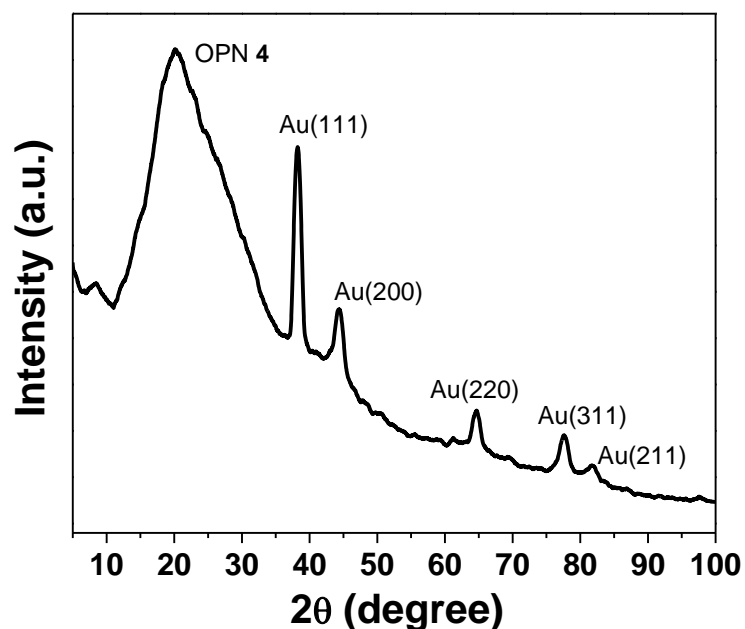


Figure S15. Powder X-ray diffraction pattern of AuNP loaded OPN **4**. Wide-angle XRD showed a characteristic broad diffraction peak at the 2θ value 20.14° indicating the amorphous nature of the polymer network. The XRD pattern further showed the diffraction peaks for the AuNPs in the OPN**4**-Au in the 2θ values of 38.0° , 44.0° , 64.5° , 77.3° and 81.8° corresponding to the {111}, {200}, {220}, {311} and {211} planes of the face-centered cubic (fcc) lattice of gold crystalline structure, respectively.^[2]

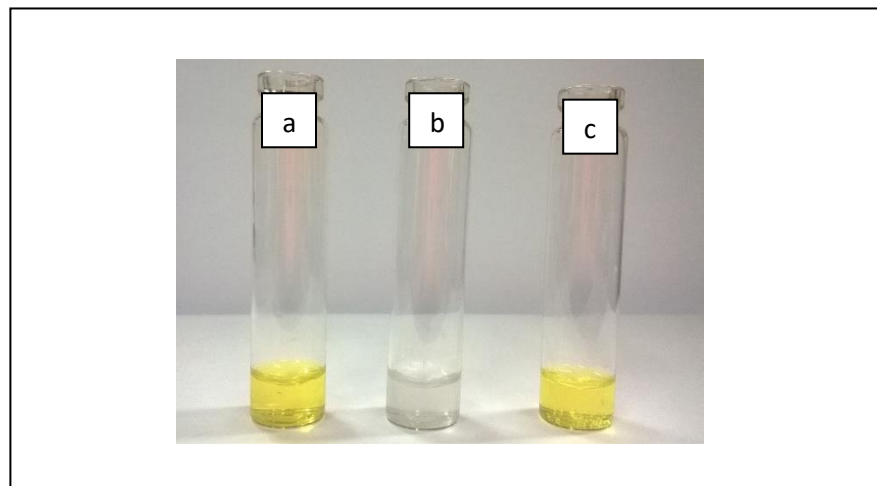


Figure S16. Reduction of 4-nitrophenol to 4-aminophenol was tested in three different experimental conditions: (a) aqueous solution of 4-nitrophenol (1.4×10^{-4} M) containing AuNP loaded OPN **4** (1 mg/mL) alone, (b) aqueous solution of 4-nitrophenol (1.4×10^{-4} M) containing both AuNP loaded OPN **4** (1 mg/mL) and sodium borohydride (0.1 M in 800 μ L) and (c) aqueous solution of 4-nitrophenol (1.4×10^{-4} M) containing sodium borohydride (0.1 M in 800 μ L) alone. The three solutions were allowed to stir for 12 h under identical condition. The reduction of 4-nitrophenol to 4-aminophenol was found to occur only for solution (b) indicating that the AuNP loaded OPN **4** is required as a catalyst for the reduction to take place by the reducing agent sodium borohydride.

Table S3. Catalytic reduction of a series of electron-rich and electron-deficient aromatic nitro compounds.^[a]

	SUBSTRATE		PRODUCT	ISOLATED YIELD %	COLOR CHANGE
ELECTRON RICH	2-Nitrophenol			95	
	3-Nitrophenol			97	
	4-Nitrophenol			99	
	4-Nitroaniline			92	
	5-Chloro-2-nitroaniline			93	
ELECTRON POOR	4-Nitrobenzoic acid		No reaction	-	
	4-Nitroacetophenone		No reaction	-	
	4-Nitrobenzaldehyde		No reaction	-	
	1-Chloro-2,4-dinitrobenzene		No reaction	-	

^[a]Substrate concentration: 0.05 mmol; Reagent: 1 mg AuNP loaded OPN **4**, 26.43 mmol NaBH₄; Solvent: ethanol-water at room temperature.

Table S4. Melting Points obtained for the purified products obtained upon the catalytic reduction experiments

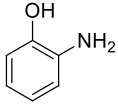
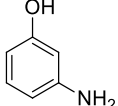
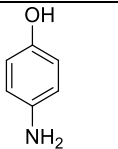
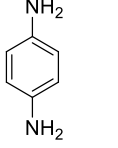
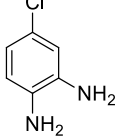
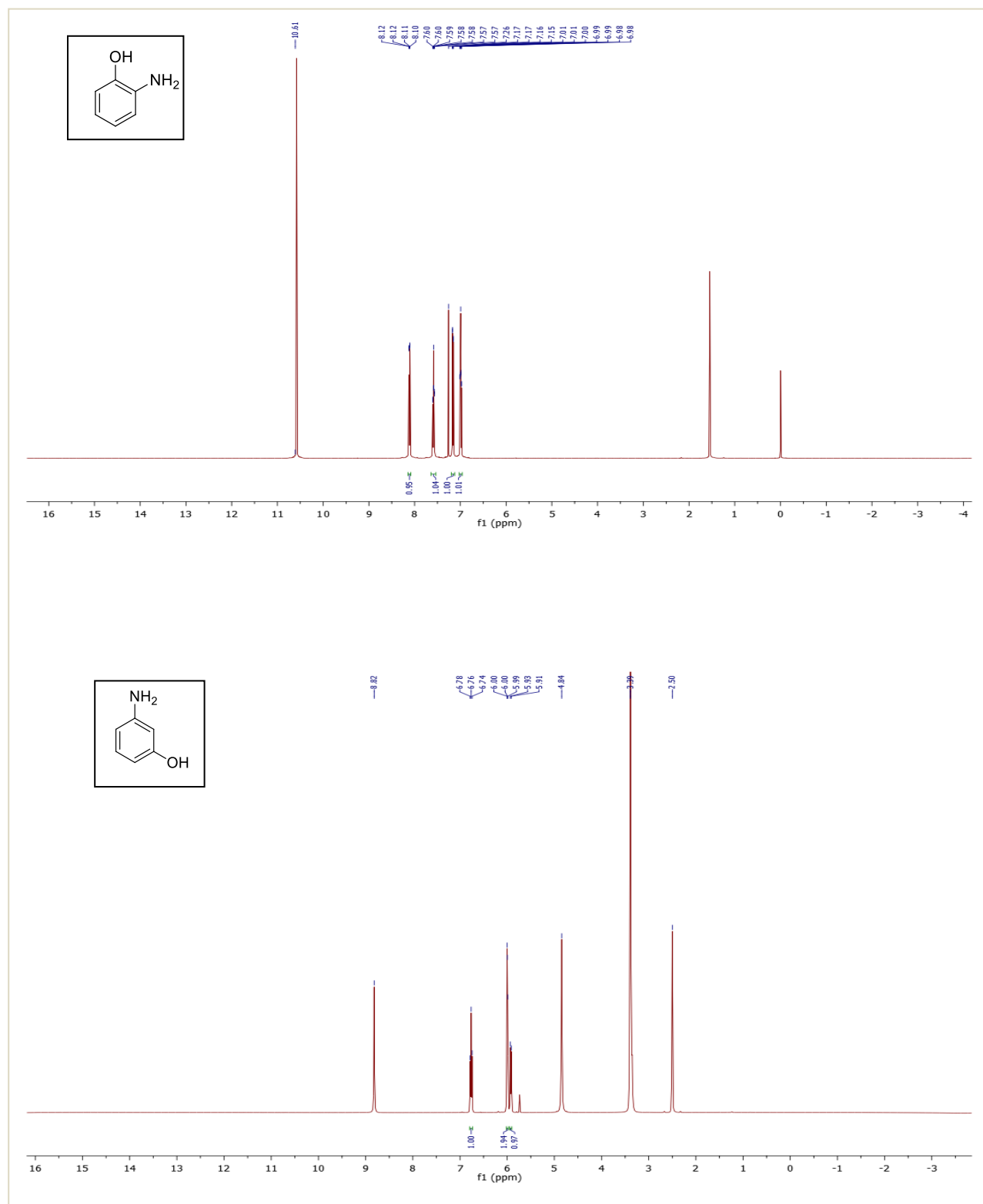
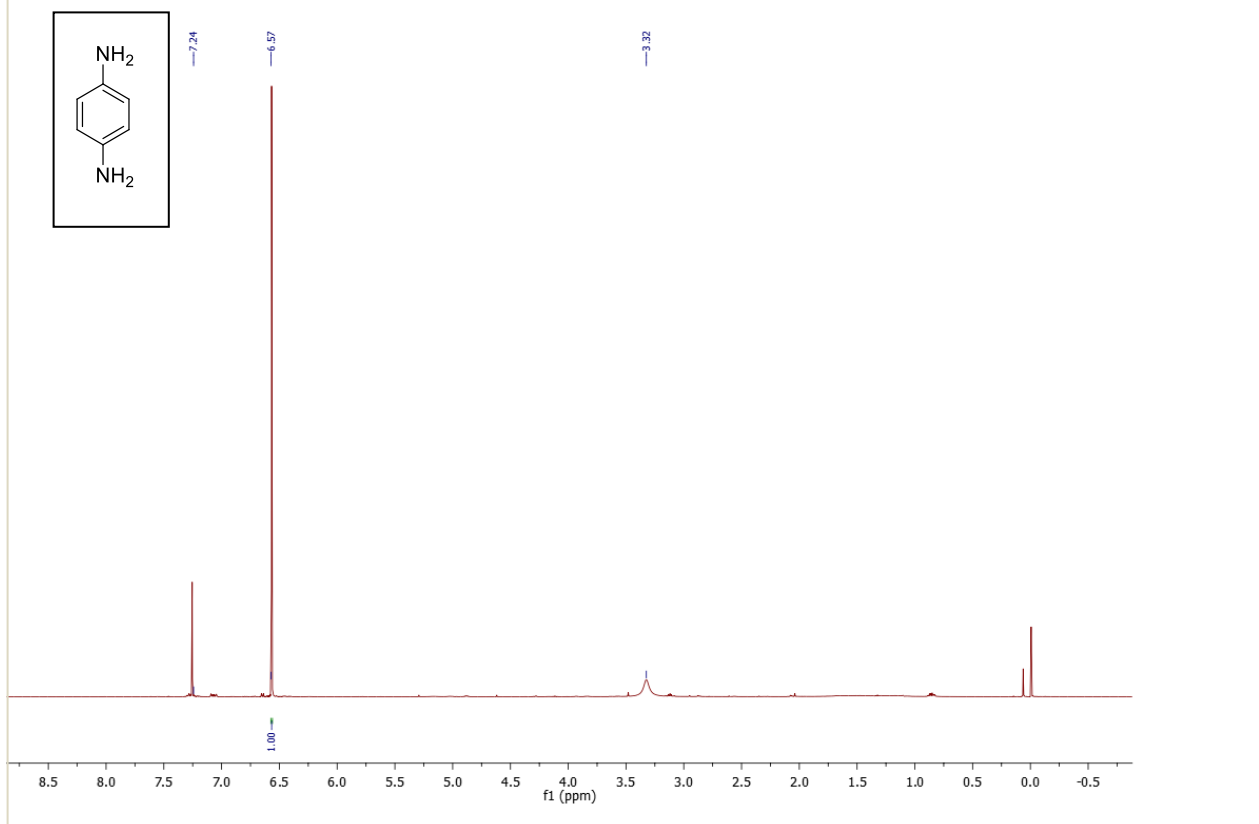
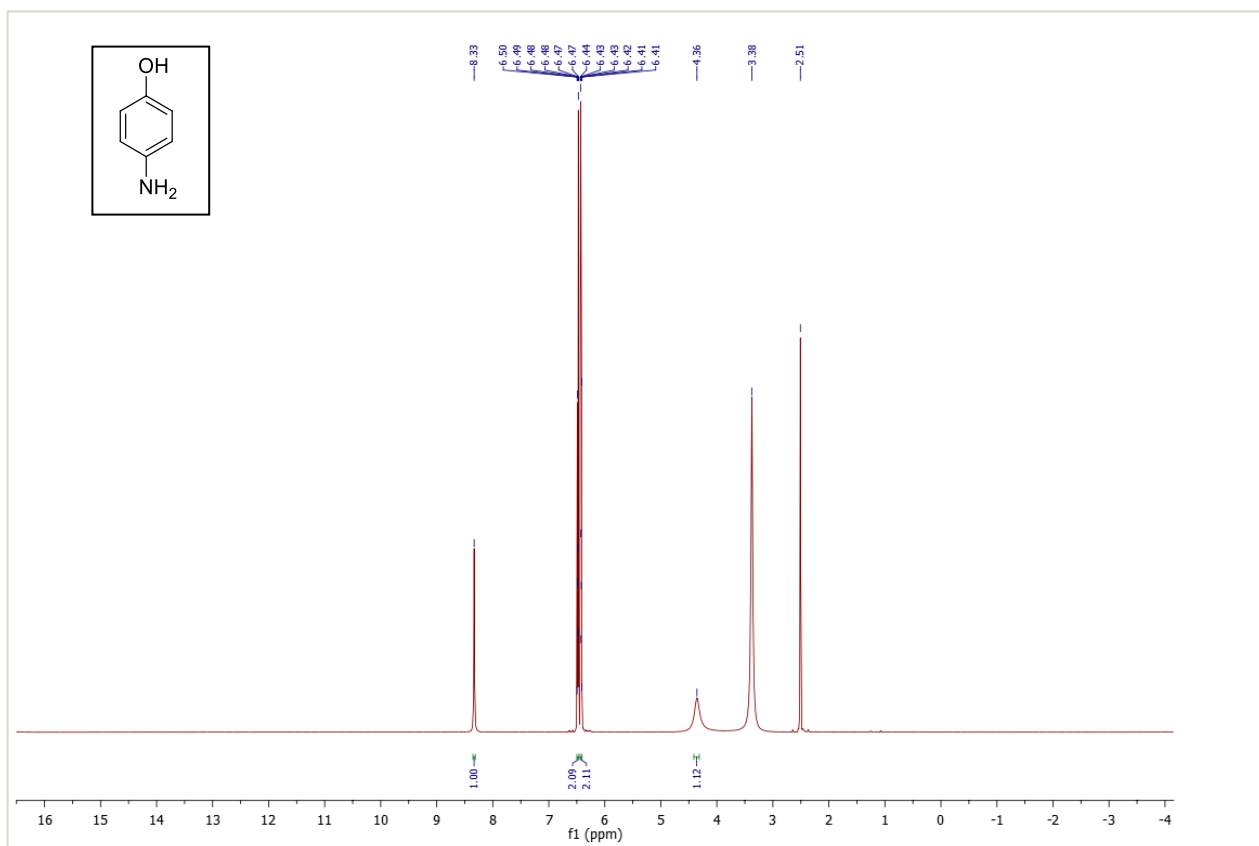
COMPOUND	MELTING POINT
	$174 \pm 1 \text{ } ^\circ\text{C}$
	$127 \pm 1 \text{ } ^\circ\text{C}$
	$186 \pm 1 \text{ } ^\circ\text{C}$
	$146 \pm 1 \text{ } ^\circ\text{C}$
	$75 \pm 1 \text{ } ^\circ\text{C}$

Figure S17. ^1H NMR spectra of the respective products of the catalytic reduction reactions.





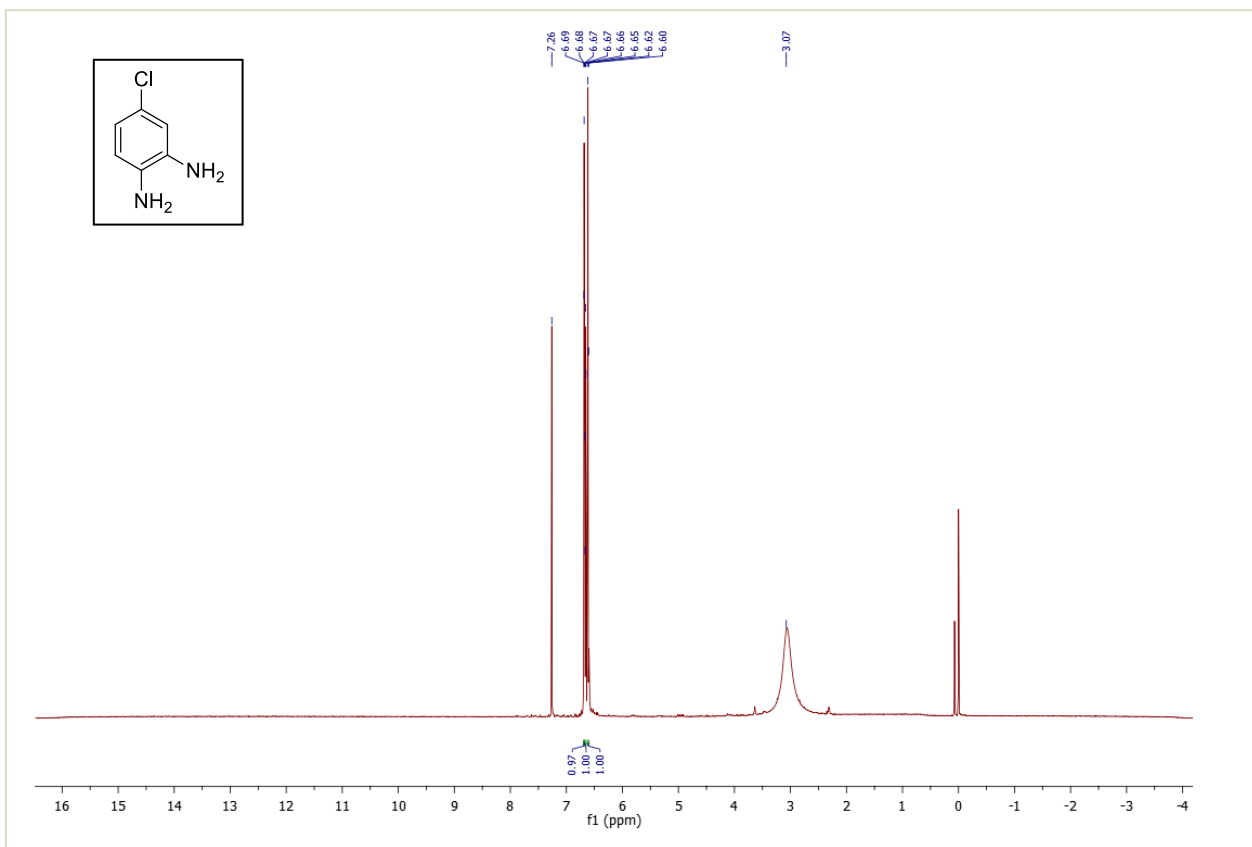
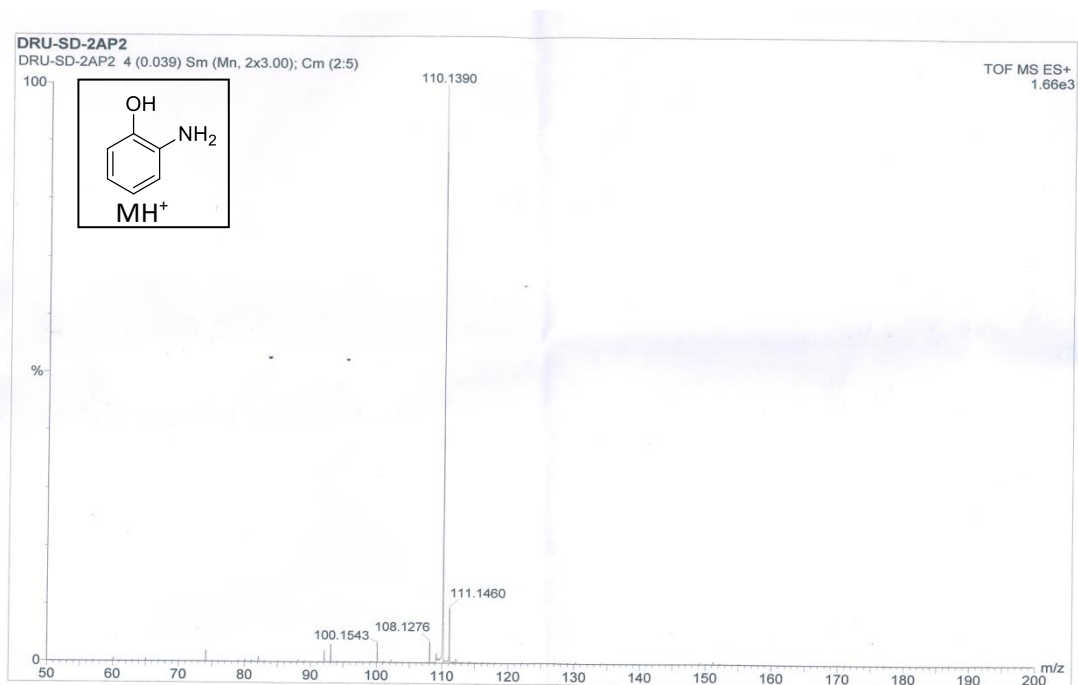
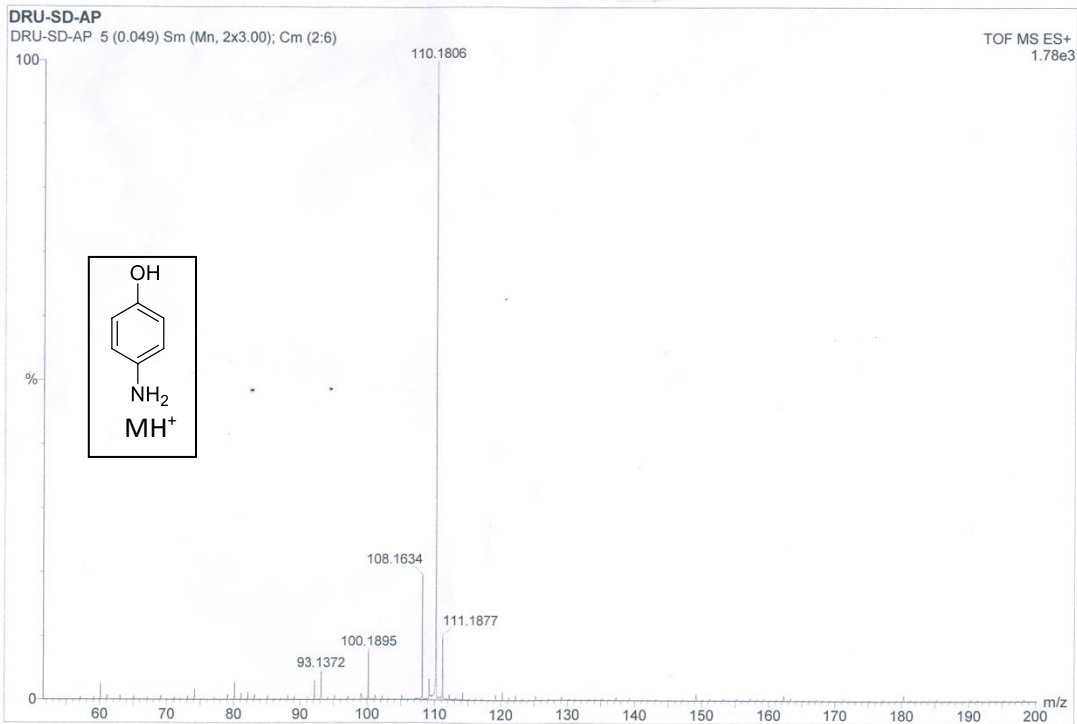
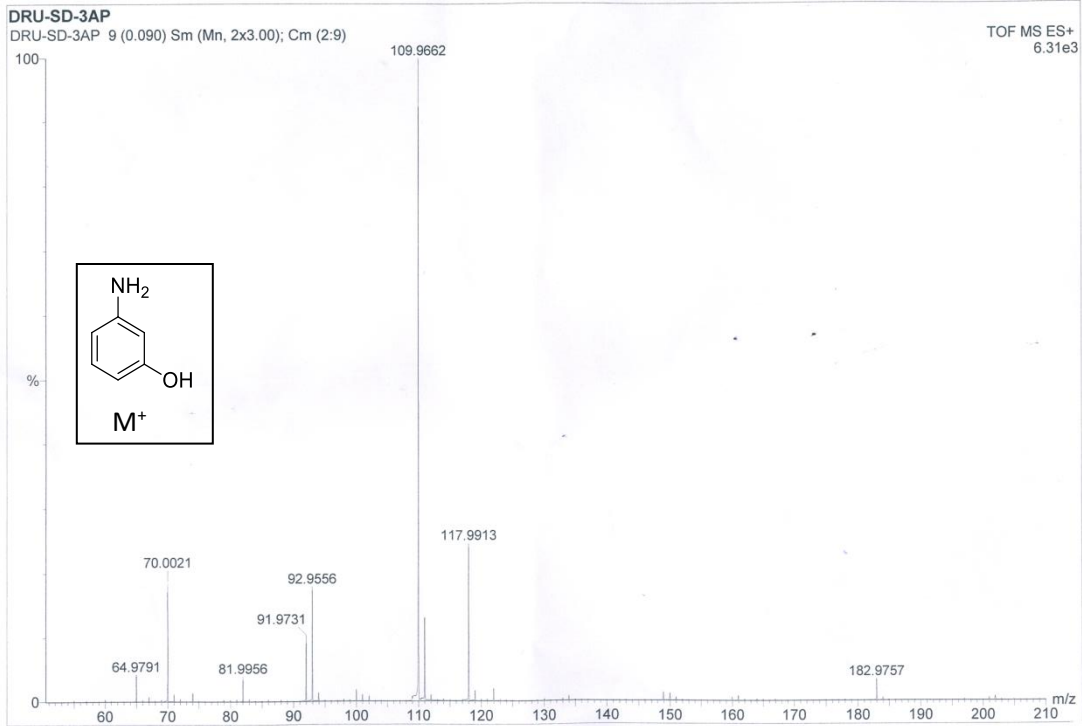


Figure S18. HRMS data of the respective products of the catalytic reduction reactions.

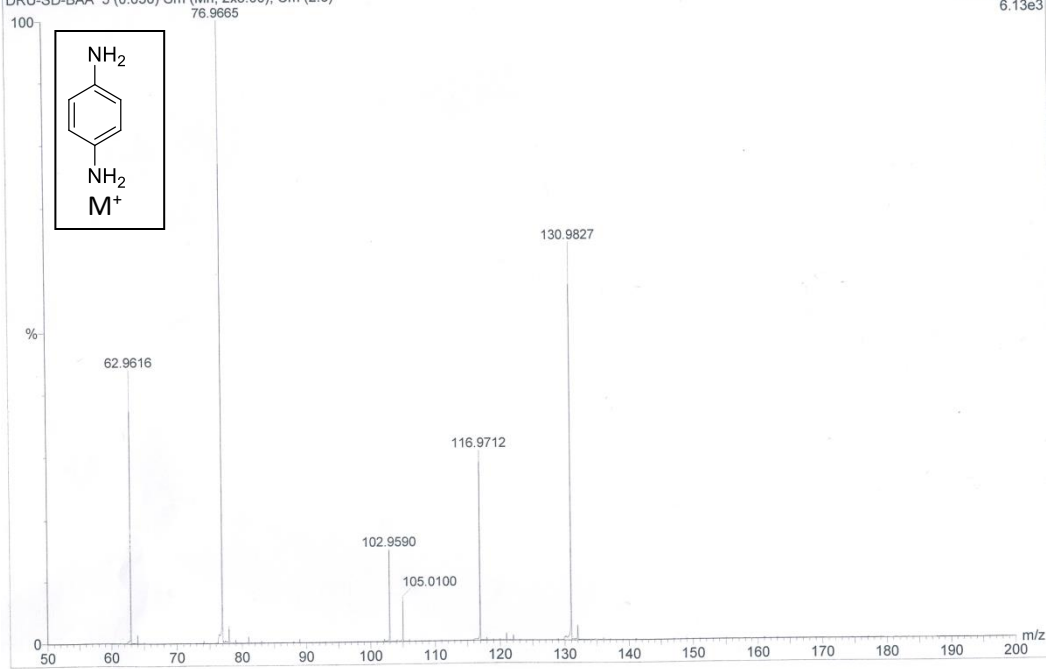




DRU-SD-BAA

DRU-SD-BAA 5 (0.050) Sm (Mn, 2x3.00); Cm (2:6)

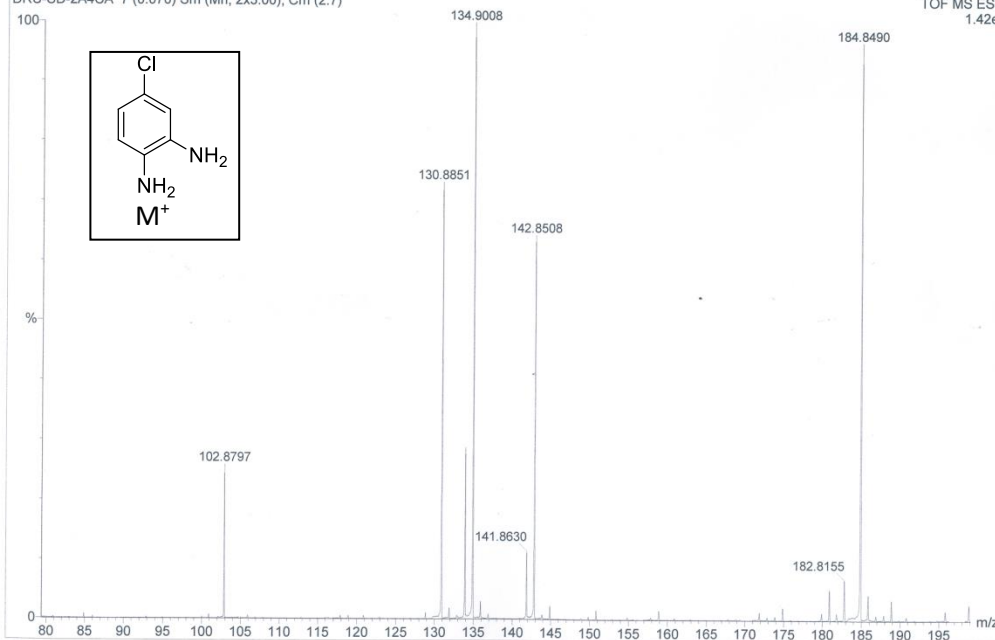
TOF MS ES+
6.13e3



DRU-SD-2A4CA

DRU-SD-2A4CA 7 (0.070) Sm (Mn, 2x3.00); Cm (2:7)

TOF MS ES+
1.42e3



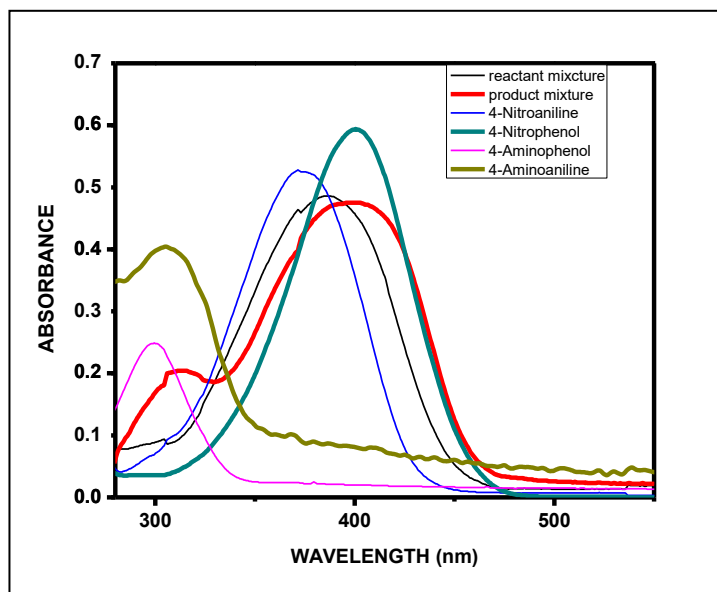


Figure S19. UV-vis spectra showing selective reduction of 4-nitroaniline by AuNP incorporated OPN **4** from a mixture of 4-nitroaniline and 4-nitrophenol in ethanol. This experiment was carried out using a 1 mL 1:1 mixture of 4-nitroaniline and 4-nitrophenol (1.4×10^{-4} M each) in ethanol. Into this mixture, 2.2×10^{-3} mM of NaBH_4 in 1 ml of distilled water was added. The UV-Vis spectra were recorded for the individual reactants and their mixtures before and after the addition of the 1 mg AuNP loaded OPN **4**. According to the results, 4-nitroaniline is reduced to *p*-phenylenediamine (peak obtained at 310 nm) and 4-nitrophenol remained unreacted (peak at 400 nm).

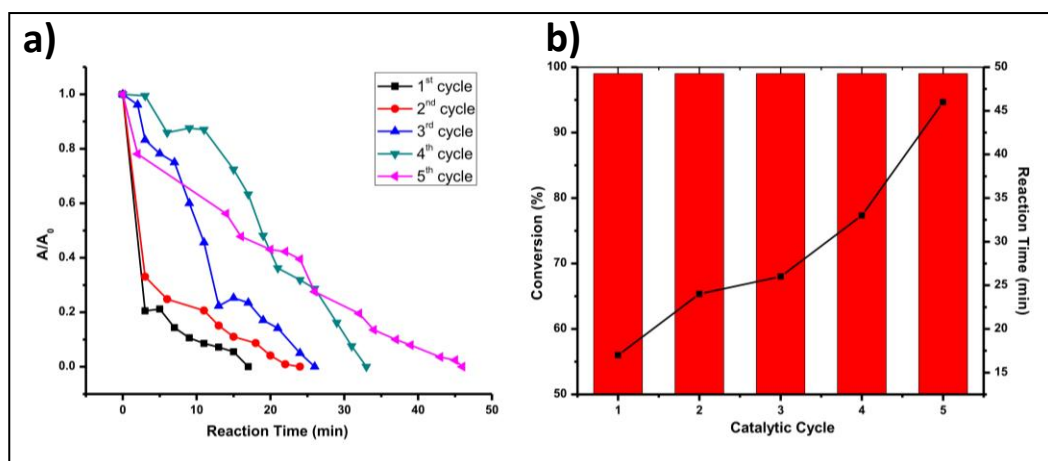


Figure S20. A set of time dependent UV-Vis experiments were performed to observe the kinetics of the reduction reaction of 4-nitroaniline to *p*-phenylenediamine by OPN 4-Au catalyst. The OPN 4-Au was recycled each time after the reduction reaction and it was reused for the next cycle of the reduction reaction. This process was repeated for a total of five times. (a) A/A_0 vs. time plot of the 5 cycles of the reduction reaction of 4-nitroaniline to *p*-phenylenediamine by OPN 4-Au catalyst. (b) Bar plot showing the time required by the OPN 4-Au catalyst to complete the reduction reaction in each catalytic cycle. Time for the 100% conversion in the 1st cycle was 17 min, 2nd cycle was 24 min, 3rd cycle was 26 min, 4th cycle was 33 min and 5th cycle was 46 min.

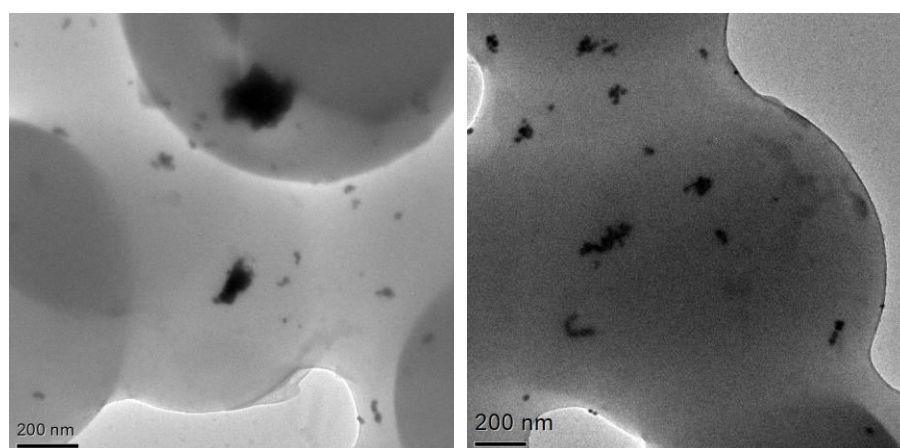


Figure S21. TEM images of AuNP loaded OPN 4 after 5th cycle of catalytic reaction. Leaching of AuNPs upon successive catalytic steps was observed, which accounts for the increased time to complete the catalytic reaction in successive cycles.

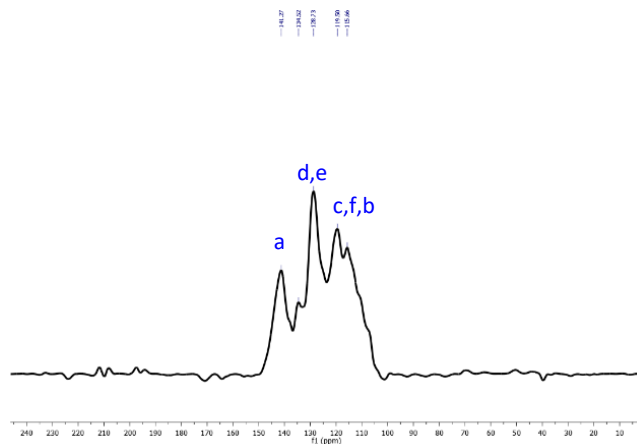


Figure S22. ^{13}C CP/MAS NMR of the recycled polymer catalyst (OPN 4 + AuNP) after 5 catalytic cycle.

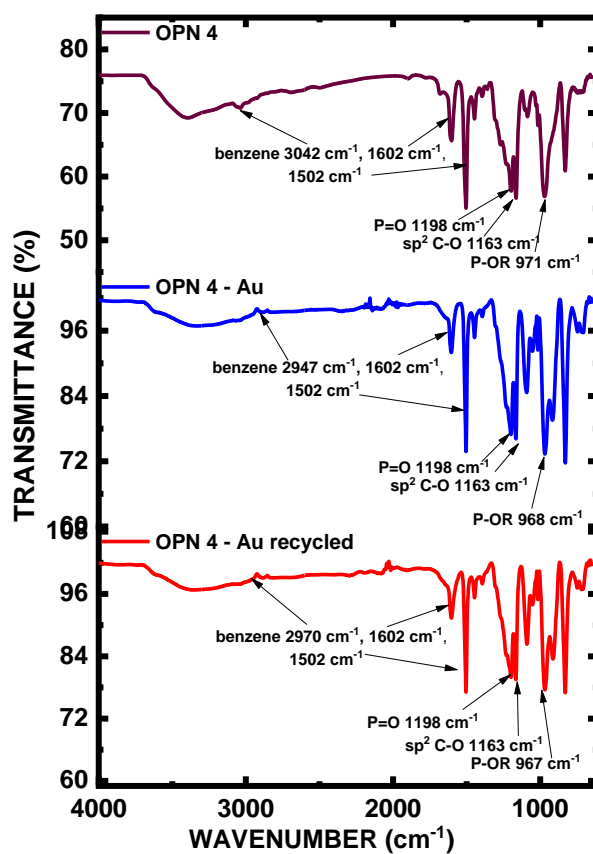


Figure S23. FTIR spectra of the recycled polymer catalyst (OPN 4 + AuNP) after 5 catalytic cycle as compared to the OPN 4 alone and as-prepared OPN 4 + AuNP.

References:

1. Gong, D.; Dong, W.; Hu, Y.; Bi, J.; Zhang, X.; Jiang, L., *Polymer*, **2009**, *50*, 5980-5986.
2. (a) Q. K. Vo, M. N. Nguyen Thi, P. P. Nguyen Thi and D. T. Nguyen, *Processes*, 2019, **7**, 631; (b) S. Siwal, N. Devi, V. K. Perla, S. K. Ghosh and K. Mallick, *Catal. Struct. React.*, 2019, **5**, 1–9.